THESIS

# ASSESSING OUTCOMES IN STRATOSPHERIC AEROSOL INJECTION SCENARIOS SHORTLY AFTER DEPLOYMENT

Submitted by

Daniel M. Hueholt

Department of Atmospheric Science

In partial fulfillment of the requirements

For the Degree of Master of Science

Colorado State University

Fort Collins, Colorado

Fall 2022

Master's Committee:

Advisor: James W. Hurrell
Co-Advisor: Elizabeth A. Barnes

Richard T. Conant

Copyright by Daniel Hueholt 2022

All Rights Reserved

ABSTRACT

ASSESSING OUTCOMES IN STRATOSPHERIC AEROSOL INJECTION SCENARIOS SHORTLY AFTER DEPLOYMENT

Current global actions to reduce greenhouse gas emissions are very likely to be insufficient to meet climate targets outlined under the Paris Agreement. This motivates performing research on possible methods for intervening in the Earth system to minimize climate risk while decarbonization efforts continue. One such hypothetical climate intervention is stratospheric aerosol injection (SAI), where reflective particles would be emitted into the stratosphere to cool the planet by reducing solar insolation. The climate response to SAI is not well understood, particularly on short-term time horizons frequently used by decision makers and planning practitioners to assess climate information. This knowledge gap limits informed discussion of SAI outside the scientific community. We demonstrate two framings to explore the climate response in the decade after SAI deployment in modeling experiments with parallel SAI and no-SAI simulations. The first framing, which we call a *snapshot around deployment*, displays change over time within the SAI scenarios and corresponds to the question "What happens before and after SAI is deployed in the model?" The second framing, the *intervention impact*, displays the difference between the SAI and no-SAI simulations, corresponding to the question "What is the impact of a given intervention relative to climate change with no intervention?" We apply these framings to annual mean 2-meter temperature, precipitation, and a precipitation extreme in the first two experiments to use ensembles of Earth system models that comprehensively represent both the SAI injection process and climate response, and connect these results to implications for other climate variables. The parallel SAI and no-SAI simulations in these experiments allow us to explore the climate response in the context of the

response to SAI, the underlying greenhouse gas forcing scenario, and the noise from internal climate variability.

# ACKNOWLEDGEMENTS

I would like to thank my co-advisors Dr. James Hurrell and Dr. Elizabeth Barnes for their insight and mentorship in my time at Colorado State University, as well as Dr. Richard Conant for serving on my graduate committee. Dr. Jadwiga Richter and Dr. Lantao Sun were insightful collaborators on the paper that makes up Chapter 2 and the Appendices of this thesis. Charlotte Connolly and Dr. Ariel Morrison provided constructive comments throughout the development of this work, and Dr. Mari Tye provided early information on useful metrics of climate extremes.

The GLENS and ARISE datasets were produced and maintained by the National Center for Atmospheric Research (NCAR). The work in this thesis was supported by the LAD Climate Fund, the Defense Advanced Research Projects Agency (grant no. HR00112290071), and the National Science Foundation Graduate Research Fellowship Program. The views, opinions, and/or findings expressed are those of the authors and should not be interpreted as representing the official views or policies of the Department of Defense or the U.S. government.

On a personal note, I am grateful to all of my friends, family, and mentors (at CSU, in NC, and elsewhere!) who have supported and worked with me throughout the last two years. Moving across the country in the middle of 2020 presented a challenging start to graduate school, and I was able to thrive because of this awesome community. I want to especially recognize Dr. Sandra Yuter at NC State University for her guidance–scientific and personal–both during and after my undergraduate studies.

TABLE OF CONTENTS

# CHAPTER 1

# INTRODUCTION

## 1.1 A BRIEF HISTORY OF CLIMATE CHANGE AND CLIMATE INTERVENTION

In 1856, Eunice Foote was the first to infer that altering the composition of Earth's atmosphere could affect global temperatures and change the climate (Foote 1856). Over the subsequent 166 years, anthropogenic climate change due to the emission of greenhouse gases by the burning of fossil fuels has become a grave threat to human society and ecological systems (e.g., Pal & Eltahir 2016, USGCRP 2018, Keys et al. 2019, Ainsworth et al. 2020, Song et al. 2021, IPCC 2021). Governments have been slow to respond to climate change, in large part due to efforts by fossil fuel companies to cast doubt on climate science (Oreskes & Conway 2011). Countries party to the United Nations Framework Convention on Climate Change established the Paris Agreement in 2015 with the goal of preventing global mean temperature from exceeding 1.5 ˚C above pre-industrial conditions (UNFCCC 2016). This goal has spurred many countries to pledge reductions in greenhouse gas emissions (e.g., Pauw et al. 2018, Depledge et al. 2022).

Despite global pledges and actions, anthropogenic climate change is anticipated to greatly surpass the Paris Agreement targets (Matthews & Wynes 2022). Consequential warming is guaranteed to occur on mid-century time horizons due to inertia within physical systems (IPCC 2021). Climate change already affects everyday climate and high-impact extreme events (e.g., Otto 2017, Fischer et al. 2021, IPCC 2021, Philip et al. 2021). Additionally, poorly-understood feedbacks within the Earth system could exacerbate climate change and its effects beyond what is anticipated in current models (e.g., Swann et al. 2010, Genet et al. 2013, Bjordal et al. 2020, King et al. 2020, Boulton et al. 2022, Weldeab et al. 2022). The United Nations

Secretary-General memorably framed the present state of the climate as signaling a “code red for humanity” (United Nations 2021).

The risks from unavoidable anthropogenic climate change motivate the study of climate intervention, broadly defined as possible methods to reduce climate risk and impacts through deliberate intervention in the Earth system. Climate intervention methods fall into two categories: solar climate intervention and carbon removal (The Royal Society 2009, National Research Council 2015). Solar climate intervention (also called “solar radiation management” or “solar geoengineering”) describes potential techniques to directly cool the planet, while carbon removal (often called “negative emissions technologies”) involves reducing atmospheric concentrations of greenhouse gases (NASEM 2019, NASEM 2021). The focus of this thesis is on the first method, specifically, the subset of solar climate intervention approaches known as stratospheric aerosol injection (SAI). SAI is a proposed method to cool the planet by injecting reflective aerosols into the stratosphere, where they would reflect away a small portion of incoming solar radiation (NASEM 2021). SAI is analogous to processes occurring naturally after volcanic eruptions (e.g., Timmreck et al. 2018).

Like the science of climate change, the study of climate intervention is not a new topic. As early as 1965, researchers speculated on the mitigation of climate impacts through methods such as spreading reflective substances over the ocean surface (Presidents Science Advisory Committee 1965). SAI, specifically, was first proposed in 1977 (Budyko 1977). However, scientific knowledge about climate intervention advanced slowly during the subsequent decades due to the fragmented nature of the research community and extensive ethical concerns around the discipline (Kintisch 2010).

A surge of interest in climate intervention began in 2006 with essays from two prominent atmospheric scientists calling for research into SAI to study its potential to minimize climate impacts and buy time for decarbonization efforts (Crutzen 2006, Wigley 2006). These

essays prompted the first coordinated modeling effort across institutions through the GEOengineering Model Intercomparison Project (GeoMIP) (Kravitz et al. 2011). GeoMIP and contemporary modeling efforts illuminated general implications of SAI, however, many models used in these experiments had poor representations of relevant parts of the Earth system and implemented SAI scenarios in highly idealized ways (Kravitz et al. 2011, Bony et al. 2013, Kwiatkowski et al. 2015, Richter et al. 2017, Bednarz et al. 2022a). SAI modeling advanced with the advent of Earth system models (e.g., Hurrell et al. 2013) capable of better representing the Earth system including the ocean, cryosphere, land, atmosphere, biogeochemistry, and interactions of these systems. The Geoengineering Large Ensemble (GLENS, Tilmes et al. 2018a) and Assessing Responses of the Assessing Responses and Impacts of Solar climate intervention on the Earth system with stratospheric aerosols (ARISE, Richter et al. 2022) projects were the first modeling experiments to use ensembles of Earth system models that simulated both the aerosol injection process and the climate response. GLENS and ARISE provided depictions of two scenarios of SAI deployment in much higher fidelity than previous experiments.

In 2021, the United States National Academies of Sciences, Engineering, and Medicine (NASEM) called for the establishment of a transdisciplinary research program on SAI and other proposed climate intervention techniques. This research program would be focused on supporting the informed discussion of climate intervention. The NASEM report identified many open research questions related to SAI relevant to the work in this thesis, including the “global- and regional-scale impacts,” and the “distribution of impacts across different parts of the world” from SAI.

### 1.2 THE PRESENT WORK

The global and regional climate responses to SAI are not well understood. This is particularly true on short-term timescales of 10 years or fewer, which are consistent with how

policymakers and planning practitioners assess climate information (e.g., Bolson et al. 2013, DePolt 2021, Pearman & Cravens 2022, Keys et al. 2022). In Chapter 2 of this thesis, we demonstrate two framings to analyze data from experiments with parallel SAI and no-SAI simulations, and apply them to GLENS and ARISE. The first framing, which we call the *snapshot around deployment,* describes the change over time in the SAI simulations and corresponds to the question "What happens before and after SAI is deployed in the model?" The second, the *intervention impact*, describes the difference between the SAI and no-SAI simulations. This corresponds to the question, "What is the impact of a given intervention relative to climate change with no intervention?" We apply these framings to 2m annual mean temperature, annual mean precipitation, and the simple intensity index (a measure of precipitation extremes) in GLENS and ARISE, while connecting these results to impacts across the Earth system.

Chapter 2, alongside Appendices A, B, and C as supplementary material, is in preparation to be submitted as the following paper:

- Hueholt, D.M., Barnes, E.A., Hurrell, J.W., Richter, J.H., Sun, L. Assessing Outcomes in Stratospheric Aerosol Injection Scenarios Shortly After Deployment. *To be submitted*.

In Chapter 3, we summarize this work and provide a discussion of some potential future directions for research.

CHAPTER 2

# ASSESSING OUTCOMES IN STRATOSPHERIC AEROSOL INJECTION SCENARIOS SHORTLY AFTER DEPLOYMENT

## 2.1 INTRODUCTION

Despite ongoing global pledges and actions to reduce greenhouse gas emissions, warming from anthropogenic climate change is expected to far exceed the targets set under the Paris Agreement (Matthews & Wynes 2022). On mid-century time horizons, substantial increases in global temperature are expected to occur both in no-mitigation pathways (Figure 1a) and in more plausible scenarios with moderate mitigation (Figure 1b) (Hausfather & Peters 2020). Near-term climate risk includes severe impacts to vulnerable communities already disproportionately affected by climate change (e.g., Shearer 2012, Carr 2016), as well as terrestrial and marine ecosystems (e.g., Frieler et al. 2013, Panetta et al. 2018, Abatzoglou et al. 2021). Poorly-understood feedbacks in Earth systems such as clouds, ice, and ecology may worsen climate change or its impacts beyond what is anticipated in current models (e.g., Swann et al. 2010, Genet et al. 2013, Bjordal et al. 2020, King et al. 2020, Boulton et al. 2022).

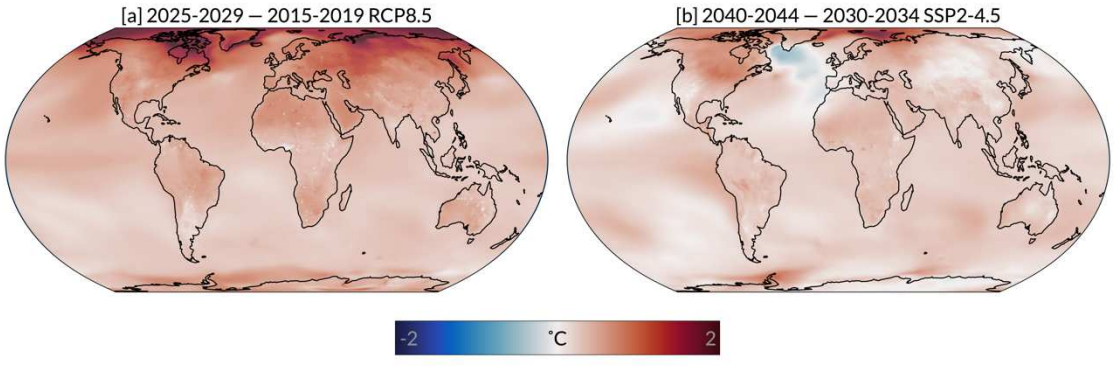


**Figure 1:** Maps of annual mean 2m temperature change between the snapshot periods in the no-SAI scenarios: RCP8.5 [a] and SSP2-4.5 [b].

These realities of unavoidable anthropogenic climate change have motivated the study of climate intervention, broadly defined as possible methods to reduce climate risk and impacts through deliberate intervention in the Earth system (The Royal Society 2009). Stratospheric aerosol injection (SAI) is one proposed climate intervention to emit reflective aerosol particles into the upper atmosphere, where the particles would reflect away some incoming solar radiation and decrease global mean temperature. SAI is inspired by processes that occur naturally after volcanic eruptions and large wildfires (e.g., Timmreck 2012, Das et al. 2021). SAI does not reduce greenhouse gas emissions, which are the root cause of anthropogenic climate change, but may complement climate change mitigation by reducing climate risk while emissions reductions and carbon removal technologies are implemented (Long & Shepherd 2014, Buck 2022). The United States National Academies of Sciences, Engineering, and Medicine (NASEM) have called for the establishment of a transdisciplinary research program on SAI and other proposed climate intervention techniques to support informed discussion of these methods (NASEM 2021).

Global and regional climate responses to SAI are not well understood. Previous SAI modeling experiments have provided useful insight into general implications of the intervention, such as the risk of rapid climate change if SAI is halted ("termination shock") and the inability of SAI to counteract impacts linked directly to $CO_2$ concentration (Jones et al. 2013, Bony et al. 2013, Kwiatkowski et al. 2015, Trisos et al. 2018). Many of these experiments (e.g., the Geoengineering Model Intercomparison Project; Kravitz et al. 2011) have relied on models with poor representations of relevant Earth system processes including atmospheric chemistry, stratospheric dynamics, and aerosol microphysics (Richter et al. 2017, Quaglia et al. 2022). The SAI scenarios in these experiments are implemented in highly idealized ways, such as by prescribing the aerosol optical depth fields or reducing the model solar constant (Kravitz et al. 2011), which can produce a very distinct climate response from when SAI is more realistically

represented with interactive aerosols (Bednarz et al. 2022a). These limitations leave large gaps in scientific knowledge of the climate response to SAI scenarios on spatiotemporal scales relevant to policymakers, planning practitioners, and questions of how SAI would affect climate risk inequality (Buck et al. 2014, NASEM 2021, Pearman & Cravens 2022).

The Geoengineering Large Ensemble (GLENS, Tilmes et al. 2018a) and Assessing Responses and Impacts of Solar climate intervention on the Earth system with stratospheric aerosols (ARISE, Richter et al. 2022) projects are the first modeling experiments using ensembles of Earth system model simulations to comprehensively represent the aerosol injection process and the climate response to SAI. GLENS and ARISE each contain parallel ensemble simulations: one following a climate change trajectory with no SAI, and one where SAI is deployed. This design helps separate the forced response to SAI from the influence of climate change and internal variability. The GLENS and ARISE projects provide high-fidelity depictions of two SAI deployment scenarios that more fully capture the global and regional climate response to SAI than previous experiments.

The parallel simulations in GLENS and ARISE provide extensive insight into the climate response to SAI, however, the plethora of data presents a challenge for effective data visualization and analysis. We propose two framings that utilize the parallel simulations of GLENS and ARISE to efficiently display multiple perspectives on the climate response to SAI. The first, which we call a *snapshot around deployment*, displays the change over time within the SAI simulations. This corresponds to the question, “What happens before and after SAI is deployed in the model?” The second, the *intervention impact*, describes the difference between the SAI and no-SAI simulations. This addresses the question, “What is the impact of a given intervention relative to climate change with no intervention?” We apply these two framings to explore the climate response to SAI in the decade after SAI is deployed in GLENS and ARISE. Decision makers and planning practitioners frequently assess climate information on

timescales of 10 years or fewer (e.g., Bolson et al. 2013, DePolt 2021, Pearman & Cravens 2022). We apply these framings to annual mean 2m temperature, annual mean precipitation, and the simple intensity index (a measure of extreme precipitation). We connect these results to global and regional impacts on an assortment of climate variables selected for their familiarity in Earth science and importance for human and ecological impacts.

Our work addresses the goals of the NASEM (2021) report to "advance knowledge relevant to decision making" and "develop policy-relevant knowledge." Consistent with this NASEM report and the broader social science literature, we explicitly distinguish our goals from research on the practical deployment of SAI about which critical ethical and governance concerns exist (Burns et al. 2016, NASEM 2021). We intend our study simply to support the informed discussion of the potential risks and benefits of SAI.

## 2.2 METHODS

### 2.2.1 DESCRIPTION OF SIMULATIONS

We use model output from the GLENS (Tilmes et al. 2018a) and ARISE (Richter et al. 2022) experiments to explore the climate response to SAI. These are the first SAI modeling experiments performed by ensembles of fully-interactive Earth system models. We summarize key aspects of the design of GLENS and ARISE, and refer readers to Tilmes et al. (2018a) and Richter et al. (2022) for more comprehensive descriptions of the experiments. Both GLENS and ARISE employ the Community Earth System Model (CESM) with the Whole Atmosphere Community Climate Model (WACCM) as its atmospheric component. WACCM includes 70 vertical layers (model top 140km) to explicitly simulate the stratosphere. GLENS and ARISE have identical 1.25˚ longitude x 0.9˚ latitude horizontal resolutions. The representation of processes thought to be most important for SAI and its climate response, including stratospheric dynamics, heterogeneous chemistry, and aerosol production, show good

agreement with observations of the mean state and anomalous conditions under volcanic aerosol loading (Mills et al. 2017, Richter et al. 2017, Gettelman et al. 2019).

Each of the two experiments contains two parallel ensemble simulations: one following a future greenhouse gas forcing scenario with no SAI, and one where SAI is also deployed. A proportional-integral feedback-control algorithm (known as the "controller") annually adjusts the amount of sulfur dioxide continuously released at four latitudes (30˚ and 15˚ N/S, all at 180˚E) intended to maintain global mean temperature, the pole-to-pole temperature gradient, and the pole-to-equator temperature gradient at some specified target value (MacMartin et al. 2014, Kravitz et al. 2017, MacMartin et al. 2017, MacMartin & Kravitz 2019). These targets ensure planetary circulations under SAI change less than if only global mean temperature were to be targeted (Tilmes et al. 2018a, Visioni et al. 2021, Cheng et al. 2022).

GLENS and ARISE depict two scenarios intended for SAI research. GLENS uses a no-mitigation emissions trajectory (Representative Concentration Pathway [RCP] 8.5; van Vuuren et al. 2011) with SAI deployed to maintain a global mean temperature target of approximately 1.2 ˚C above pre-industrial conditions (Tilmes et al. 2018a). This yields a large signal-to-noise ratio useful to isolate the forced response to the SAI intervention over time. ARISE is run with a moderate-mitigation scenario (Shared Socioeconomic Pathway [SSP] 2-4.5; Riahi et al. 2017) and a temperature target of 1.5 ˚C above preindustrial. ARISE illustrates one plausible future where the use of SAI complements current mitigation strategies to achieve Paris Agreement goals (Richter et al. 2022). There are fundamental differences between the experimental design of GLENS and ARISE. We summarize these in Table 1, and provide details on their implications here.

1. **The two experiments use different model versions:** GLENS uses CESM1(WACCM5) while ARISE uses CESM2(WACCM6). Thus, GLENS and ARISE exhibit different spatial patterns of the forced response due to model dependencies, particularly the

depiction of subtropical and Southern Ocean low clouds (Gettelman et al. 2019, Fasullo & Richter 2022). CESM1 is described by Hurrell et al. (2013) and CESM2 by Danabasoglu et al. (2020).

2. **The two experiments have different forcing scenarios:** GLENS uses RCP8.5 while ARISE uses SSP2-4.5, which yields distinct spatial patterns of the forced response. RCP8.5 and SSP2-4.5 differ in many ways that affect these spatial patterns, including the depiction of land use and aerosol emissions, but the primary influence is the different $CO_2$ concentration which operates through a direct effect on clouds and precipitation (e.g., Sherwood et al. 2015, Rugenstein et al. 2016, Fasullo & Richter 2022). These scenario dependencies are largest in the mid-latitudes and subtropics (Fasullo & Richter 2022).
3. **The global mean temperature target is ~1.2 ˚C above preindustrial in GLENS, while it is 1.5 ˚C in ARISE; SAI is deployed in 2020 in GLENS and 2035 in ARISE.** The impacts due to differences in temperature target and deployment year are not well understood. Targeted modeling experiments to provide insight into these parameters have recently been completed (MacMartin et al. 2022), but no formal analysis of these simulations has yet been published.
4. **The Atlantic Meridional Overturning Circulation (AMOC) increases through the simulation in GLENS but decreases in ARISE**. The ocean state in GLENS is branched off of a single member of the CESM Large Ensemble (Kay et al. 2015) in which the AMOC is strengthening. Thus, each realization of GLENS begins with a strengthening state of the AMOC. On the decadal time horizons we emphasize in this study, the memory of these ocean initial conditions has not fully dispersed (Tilmes et al. 2018a, Fasullo et al. 2018). This increases heat transport into the North Atlantic and influences European climate (Fasullo et al. 2018). Longer-term trends in AMOC

strength may be caused by changes in precipitation that impact salinity and temperature gradients in the ocean (Fasullo & Richter 2022). The ocean state in ARISE is branched off of five separate SSP2-4.5 simulations which have dispersed over multiple decades (Richter et al. 2022). Thus, ARISE samples ocean internal variability more widely than GLENS.

5. **Aerosol is injected at higher altitudes in GLENS (~25 km) than in ARISE (~21 km)**. Injection height affects stratospheric chemistry, but has few other effects on the climate as long as the altitude is above the tropopause (Tilmes et al. 2018b, Zhang et al. 2022). Injection heights near 20 km are consistent with near-future aerospace technology (D'Oliveira et al. 2016, Moriyama et al. 2017, Smith et al. 2022).

**Table 1:** Contrasts key aspects of the experimental design of GLENS and ARISE. Compiled from Tilmes et al. (2018a) and Richter et al. (2022).

| | **GLENS** | **ARISE** |
|---|---|---|
| **Model version** | CESM1(WACCM5) | CESM2(WACCM6) |
| **Ensemble size (SAI)** | 21 members from 2020-2099 | 10 members from 2035-2069 |
| **Ensemble size (no-SAI)** | 21 members from 2010-2030, 3 from 2010-2097 | 5 members from 2015-2069, 5 from 2015-2100 |
| **Forcing scenario** | RCP8.5: No mitigation | SSP2-4.5: Moderate mitigation |
| **Global mean surface temperature target** | ~1.2 ˚C above preindustrial (model value in the year 2020) | 1.5 ˚C above preindustrial (model mean 2030-2039) |
| **Temperature gradient targets** | 2010-2030 mean | 2020-2039 mean |
| **SAI deployment year** | 2020 | 2035 |
| **Injection height** | ~25 km | ~21 km |

Because the controller maintains meridional temperature gradient targets under different spatial patterns of the forced response, it injects aerosol in disparate latitudinal amounts throughout the simulation in each experiment. This leads to distinct global distributions of aerosol optical depth (Figure 1 in Fasullo & Richter 2022) with corresponding

differences in the regional climate response. GLENS and ARISE can be contrasted in generalities to illuminate the differences in the climate response produced by two SAI scenarios simulated in physically comprehensive models. However, unless the model dependencies and scenario dependencies themselves are of interest, it is not appropriate to directly, quantitatively compare a given variable across GLENS and ARISE.

### 2.2.2 ANALYSIS METRICS

We use the five years prior to SAI deployment (2015-2019 in GLENS, 2030-2034 in ARISE) as pre-intervention reference periods, and the five-year period beginning five years after deployment (2025-2029 in GLENS, 2040-2044 in ARISE) as a post-intervention reference period while remaining close to the deployment year. The ensemble sizes of the GLENS and ARISE experiments (Table 1) increase the number of years available for analysis, allowing us to average over many realizations of relatively short spans of time (Deser et al. 2012, Maher et al. 2021, Tebaldi et al. 2021). We develop two framings to investigate the climate response to SAI. Our first framing, which we call a *snapshot around deployment*, depicts change over time within the SAI experiments: the difference between 2025-2029 and 2015-2019 in GLENS, and 2040-2044 and 2030-2034 in ARISE. This can be phrased as answering the question: “What happens before and after SAI is deployed in the model?” Our second framing, the *intervention impact*, is the SAI and no-SAI difference for the 2025-2029 period in GLENS and the 2040-2044 period in ARISE. This can be expressed as answering the question: “What is the impact of a given intervention relative to climate change with no intervention?” This was inspired by the “world avoided” perspective used to study the Montreal Protocol (e.g., Morgenstern et al. 2008).

We structure our framings to focus on the short-term climate responses occurring in the first 10 years after SAI deployment. This near-term timeframe has been analyzed with respect to the atmospheric dynamical response to SAI (e.g., Tilmes et al. 2017, Richter et al. 2018), but has seen little exploration with respect to climate impacts. Policymakers and planning practitioners

often assess climate information on short-term time horizons of 10 years or fewer (e.g., Bolson et al. 2013, DePolt 2021, Pearman & Cravens 2022, Keys et al. 2022). Thus, we portray our results consistently with how information could hypothetically be used for decisions about SAI deployment, governance, and evaluation. The signal-to-noise ratio of the forced response to SAI is smaller on this time horizon than when trends are calculated over a longer span of time. We use timeseries (Figure 2) to complement ensemble mean global maps of our two framings (Figures 3-8). These allow us to display the longer-term evolution of a variable and emphasize the contribution of internal variability for a specific region. We show timeseries for 2010-2069 to span the period where output from both GLENS and ARISE are available.

As an Earth system model, CESM provides a breadth of model output including variables that represent the atmosphere, ocean, land surface, and ecology. This allows for many aspects of the climate response to SAI to be assessed holistically. We examined a wide variety of variables in developing this paper. Here, we present a subset that are familiar in Earth science, have links to human impacts, and whose representation in CESM has been evaluated against observations (Hurrell et al. 2013, Danabasoglu et al. 2020, Fasullo 2020). We describe our selected variables below.

- **Temperature:** We calculate annual mean 2-meter temperature from monthly output. For temperature and all other variables, we define regions following the IPCC Working Group 1 Fifth Assessment Report Annex (van Oldenborgh et al. 2013), except when specified otherwise. We illustrate the regions we discuss in this work in Figure C1. In addition to the regions highlighted in Figure 2, we provide timeseries of 2-meter annual mean temperature for all IPCC-defined regions in Appendix B.
- **Tropical nights:** We use tropical nights from the World Climate Research Program's Expert Team on Climate Change Detection and Indices (ETCCDI) set of extreme indices as an example of a temperature extreme. Tropical nights is the annual count of days

where minimum temperature exceeds 20 ˚C (68 ˚F) (Zhang et al. 2011). High nighttime temperatures increase mortality, particularly in urban areas without widespread air conditioning (Buechley et al. 1972, Sillmann & Roeckner 2008, Laaidi et al. 2012, Rathi et al. 2021). We calculate tropical nights from daily minimum temperature using Pyclimdex (Groenke 2020/2022). Tye et al. (2022) comprehensively explore ETCCDI extremes in GLENS; no such assessment has been completed for ARISE.

- **Sea surface temperature (SST):** We calculate annual mean SST from monthly output at the surface level of the ocean component in CESM.
- **Marine heatwaves:** We identify marine heatwaves as events where daily mean SST exceeds the daily local 90th percentile (computed over 2010-2020) for longer than 5 days (Hobday et al. 2016, Oliver 2015/2022). This definition is standard in public communication and the scientific literature (e.g., Benthuysen et al. 2018, Holbrook et al. 2020, MHIWG 2022). Marine heatwaves occur at many locations around the world (Smith et al. 2021), and we select a point in the Leeuwin Current (30.63˚S, 112.5˚E) where they have been frequently observed to harm local ecology (Chandrapavan et al. 2019, Holbrook et al. 2020). We apply a left-aligned 5-year rolling sum of days with marine heatwaves to smooth interannual variability in Figure 2l.
- **Sea ice extent:** We show sea ice extent in its minimum month for both hemispheres–September for the Arctic and February for the Antarctic (Stroeve et al. 2012, Parkinson 2019). Sea ice extent is the sum of grid cell areas with ice fraction greater than 0.15 in the atmospheric component of CESM (NSIDC 2020).
- **Precipitation:** We derive annual mean precipitation from monthly total precipitation. To describe South Asian Monsoon rainfall, we use the conventional dynamical definition of June through September mean precipitation between 10˚N to 40˚N and 80˚E to 100˚E

(Geen et al. 2020). We provide timeseries of annual mean precipitation for all IPCC-defined regions in Appendix B.

- **Simple intensity index:** We use the ETCCDI simple intensity index to illustrate changes in a precipitation extreme. The simple intensity index measures the precipitation amount divided by the number of days with precipitation (Zhang et al. 2011). This is a standard metric to analyze trends in precipitation intensity (e.g., Alexander et al. 2006, Ayugi et al. 2021). Following Ayugi et al. (2021), we define the East African region as spanning 12˚S to 5˚N and 28 ˚E to 42˚E to capture relevant regional climate features. We highlight East Africa due to its high exposure to extreme precipitation events (Adhikari et al. 2015, Nicholson 2017, Wainwright et al. 2021), and include additional timeseries of the simple intensity index for all IPCC-defined regions in Appendix B. We calculate the simple intensity index using Pyclimdex (Groenke 2020/2022).

Regional trends in the model output are due to combinations of the forced response to the SAI intervention, the direct effects of $CO_2$ concentration, and internal variability (Fasullo & Richter 2022). We use a metric based on the spread of the parallel ensemble simulations in GLENS and ARISE to evaluate where the signal from the SAI intervention is or is not robust relative to contributions from other sources. We detail the calculation of this metric, which we call *robustness*, in Appendix A. In the text of this work, we refer to results with high robustness as "robust." Maps of robustness for each figure discussed in the Results section are displayed in Figure C2. These figures can be used to assess robustness visually by interpreting areas colored in yellow or green as being robust, while grayscale colors ("muted" regions, Tomkins et

al. 2022) are not robust.

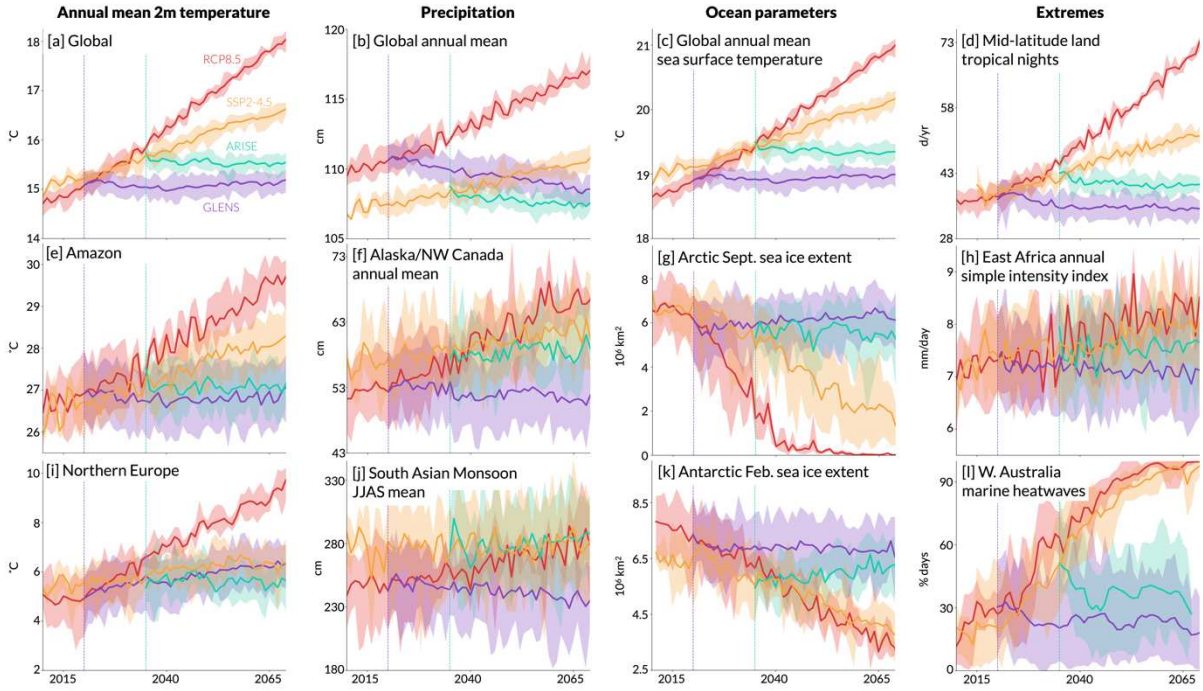


**Figure 2:** Timeseries of selected climate variables in the GLENS and ARISE experiments. Bold line shows the ensemble mean for each scenario; shading illustrates the range of the ensemble members given by the maximum and minimum values at each year. The vertical dashed lines mark the deployment of SAI in 2020 (GLENS) and 2035 (ARISE). See Methods for detailed descriptions of variables and regions.

## 2.3 RESULTS

GLENS and ARISE both maintain global mean temperature at their respective target values, while the no-SAI RCP8.5 and no-SAI SSP2-4.5 scenarios continue warming globally throughout the period (Figure 2a). Thus, global mean temperature shows a clear forced response to the SAI intervention. For each timeseries shown in Figure 2, the envelope around the ensemble mean illustrates a range of internal climate variability by spanning the maximum to minimum member at each year. The ensemble sizes for each scenario differ and are given in Table 1. While forced trends are visible in the ensemble mean for many of the timeseries (Figure 2), internal climate variability is substantial especially for regional scales and noisier variables such as precipitation (e.g., Figure 2h). The ensemble spreads of the SAI and no-SAI scenarios overlap for all quantities in the time periods shortly after deployment when the forced response is small. Thus,

internal variability can mask the forced response to the SAI intervention for any individual realization–especially on short time horizons (Keys et al. 2022).

We use global maps corresponding to the *snapshot around deployment* and *intervention impact* framings (Figures 3-8, see Methods for details) to explore the ensemble mean response of temperature, precipitation, and the simple intensity index within the decade after SAI deployment. We refer to timeseries in Figure 2 to connect results from our framings to the evolution of a variable over a longer period of time and to display the spread due to internal variability.

### 2.3.1 WHAT HAPPENS BEFORE AND AFTER SAI IS DEPLOYED IN THE MODEL?

We begin our discussion with 2-meter temperature (Figure 3), as it is the variable directly targeted by the SAI intervention. Some global warming is visible in the GLENS snapshot due to the rapid warming rate in the underlying RCP8.5 emissions trajectory. The GLENS experimental design halts global mean temperature at 2020 levels, which leaves some warming relative to the 2015-2019 mean which defines our pre-intervention snapshot baseline. The SSP2-4.5 forcing scenario used in ARISE yields a much more moderate rate of warming as compared to RCP8.5 and a smaller relative change between the 2030-2034 baseline and the deployment of SAI in 2035. Hence, the snapshot around deployment for ARISE does not display substantial planetary-scale warming.

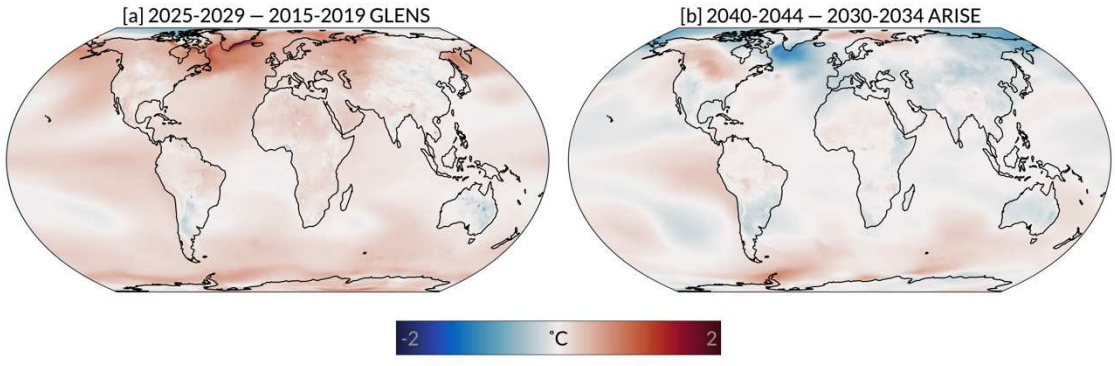


**Figure 3:** Maps of annual mean 2m temperature change between the snapshot periods within the SAI scenarios: GLENS [a] and ARISE [b].

The subpolar North Atlantic Ocean stands out as the region experiencing the largest temperature trends (Figure 3). The sign of the trend is opposite in each experiment: warming in GLENS (Figure 3a), but cooling in ARISE (Figure 3b). This difference is driven by the opposite-signed AMOC evolution in GLENS and ARISE. The strengthening AMOC throughout the simulation period in GLENS increases heat transport into the North Atlantic (Fasullo et al. 2018); in contrast, the AMOC weakens in ARISE (Richter et al. 2022). These trends in the AMOC are likely due to memory of the ocean initial conditions on the short timescales shown in the snapshot around deployment (Tilmes et al. 2018a, Fasullo et al. 2018). On a longer time horizon, the direct effect of $CO_2$ concentration on precipitation may drive a forced response in the AMOC by altering oceanic salinity and temperature gradients (Fasullo & Richter 2022), however, this long-term effect would not be visible in our snapshot around deployment.

In general, regional changes in annual mean 2m temperature after SAI deployment are much smaller in GLENS and ARISE (Figure 3) than in no-SAI RCP8.5 and no-SAI SSP2-4.5 (Figure 1). All regions (save Northern Europe in GLENS, discussed shortly) defined by the IPCC WG1-AR5 Atlas (van Oldenborgh et al. 2013) have a similar temperature response over time to the global mean. We provide 2m annual mean temperature timeseries for each IPCC region in the Appendix B to illustrate the universality of this response. We highlight the Amazon region (Figure 2e) as an example of the typical evolution of annual mean temperatures on a regional scale. The response in the Amazon is very similar to the global response: GLENS and ARISE are maintained near their pre-deployment values, while the no-SAI scenarios continue to warm through the period. Temperature trends are robust for all land area in GLENS, and almost all land area in ARISE (Figure C2a,b). A description of the metric we use to assess robustness of trends can be found in Appendix A.

Northern Europe (Figure 2i) is the sole IPCC-defined region to experience sustained surface warming after deployment in any of the SAI scenarios. This region undergoes moderate

warming throughout the period in GLENS. One cause of this warming may be a forced positive trend in the North Atlantic Oscillation driven by stratospheric heating from the absorption of radiation by the sulfate aerosols injected by the SAI intervention (Banerjee et al. 2021). The strengthening AMOC could also contribute to this regional warming by importing heat from lower latitudes (Fasullo et al. 2018). Northern European warming does not occur in ARISE (Figure 2i, 3b), which requires a smaller amount of aerosol injection to maintain its climate goals against a more moderate radiative forcing than in GLENS. This lower aerosol burden results in less stratospheric heating which reduces the corresponding circulation response (Bednarz et al. 2022b). The SSP2-4.5 radiative forcing after 2100 becomes comparable to mid-century RCP8.5 (Meinshausen et al. 2020), and the aerosol injected on these timescales could induce a more substantial circulation response via stratospheric heating. The differing responses in Northern Europe emphasize that climate responses in an individual scenario may be particular to that strategy, and cannot be assumed to be general features of all SAI interventions.

We now turn to the snapshot around deployment for precipitation (Figure 4). The ITCZ shifts southward in both GLENS and ARISE (Figure 4). While this trend is robust in GLENS (Figure C2c), it is less so in ARISE (Figure C2d). The controller in GLENS and ARISE minimizes the magnitude of the perturbation to the ITCZ by maintaining the pole-to-pole and pole-to-equator temperature gradients which strongly influence ITCZ location (Kang et al. 2018, Undorf et al. 2018, Cheng et al. 2022). However, the controller does not target every factor that influences the ITCZ location, which include differences in the relative aerosol burden between the Northern and Southern Hemispheres and changes in heat transport by the AMOC (Haywood et al. 2013, Iles & Hegerl 2014, Moreno-Chamarro et al. 2019, Ciemer et al. 2021). Thus, GLENS and ARISE reduce but cannot fully eliminate their respective perturbations to the ITCZ location (Cheng et al. 2022). Targeted modeling experiments and observations after volcanic eruptions

indicate that much larger ITCZ migrations are possible under SAI strategies that do not consider hemispheric temperature gradients (Haywood et al. 2013, Cheng et al. 2022).

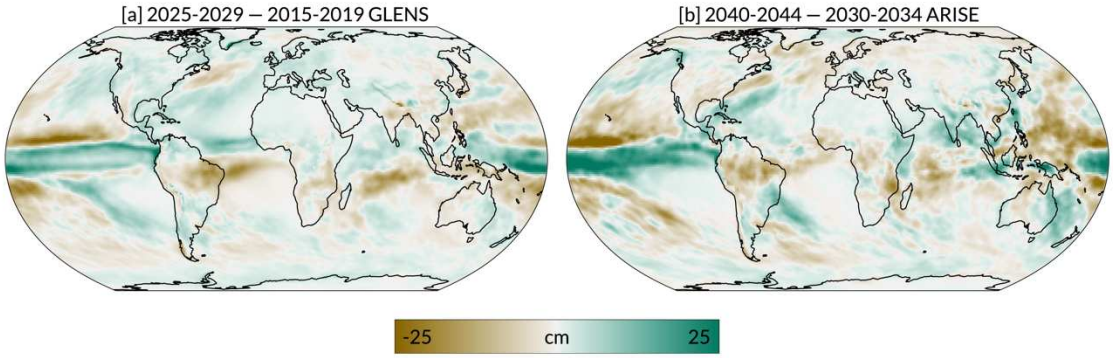


**Figure 4:** Maps of annual mean precipitation change between the snapshot periods within the SAI scenarios: GLENS [a] and ARISE [b].

Precipitation decreases over much of the western Pacific in GLENS and ARISE (Figure 4). While this change is not robust during the decade immediately after SAI deployment, a sustained trend eventually emerges in GLENS and is responsible for a decrease in globally-averaged precipitation throughout the simulation (Figure 2b). Since these changes primarily affect precipitation over the ocean, land-only precipitation trends in GLENS are small (Figure C3). The decrease in tropical oceanic precipitation may be related to the direct effect of $CO_2$ concentration in the RCP8.5 emissions pathway or the circulation response to stratospheric heating, but the precise underlying dynamics are not well understood (Bony et al. 2013, Simpson et al. 2019). Changes in global precipitation over time in ARISE are difficult to identify (Figure 2b), which indicates a more moderate injection strategy may minimize impacts on the global hydrologic cycle.

Early modeling results indicated certain SAI strategies could cause large decreases in South Asian Monsoon precipitation (Robock et al. 2008). Any changes to the monsoon directly affect water availability and agricultural productivity in a densely populated region, with further impacts on global food supply (Gadgil & Rupa Kumar 2006, Kulkarni et al. 2016). South Asian Monsoon precipitation robustly decreases in GLENS (Figure 4a), although the magnitude of the

change is smaller than the increase throughout the period in no-SAI RCP8.5 (Figure 2j). Late in the century in GLENS, monsoon failures double in frequency due to circulation changes induced by stratospheric heating from the enormous aerosol burden (Simpson et al. 2019). In contrast, South Asian Monsoon precipitation remains largely unchanged in both SSP2-4.5 and ARISE. Thus, impacts on monsoon precipitation are dependent on the SAI strategy rather than a general feature of this type of intervention.

On our short time horizon of the decade after deployment, global changes in the simple intensity index are very noisy with small changes seen overall. The largest regional feature is a decrease in the simple intensity index in Western Australia in ARISE (Figure 5b). When examined over the 2035-2069 period, it appears this is a transient anomaly likely due to internal variability (Figure C4). Precipitation extremes exhibit the largest internal variability of any quantity examined here. The 10-member ensemble of ARISE is not sufficient to isolate the forced response to SAI on precipitation extremes for regional spatial scales and short timescales. An ensemble size of 40 members or more may be necessary to reliably isolate these forced trends (Kirchmeier-Young & Zhang 2020).

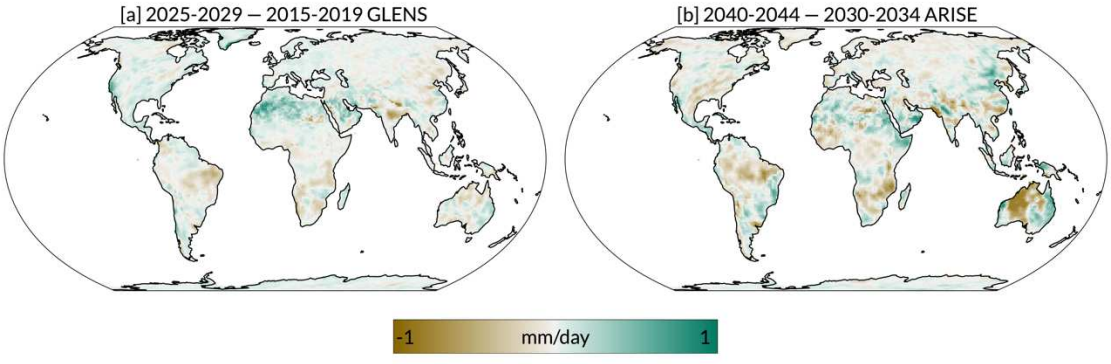


**Figure 5:** Maps of annual mean simple intensity index change between the snapshot periods within the SAI scenarios: GLENS [a] and ARISE [b].

### 2.3.2 WHAT IS THE IMPACT OF A GIVEN INTERVENTION RELATIVE TO CLIMATE CHANGE WITH NO INTERVENTION?

GLENS and ARISE both avert warming around the globe (Figure 6); that is, they robustly remain cooler than their respective no-SAI scenarios (Figure C2a, Figure C2b). This impact is evident even in the decade immediately following deployment and is nearly single-signed worldwide (Figure 6). The Arctic experiences the greatest averted warming (Figure 6), because the controller greatly reduces Arctic amplification by maintaining the pole-to-equator temperature gradient in addition to global mean temperature. In either GLENS or ARISE, no regions experience robust warming relative to climate change in the ensemble mean. Regions that warm relative to a pre-intervention baseline, namely Northern Europe in GLENS, still experience averted warming relative to climate change (Figure 6a). This illustrates the value of using our two framings together: the snapshot around deployment shows the tangible climate response, while the intervention impact places these changes in context to climate change with no SAI.

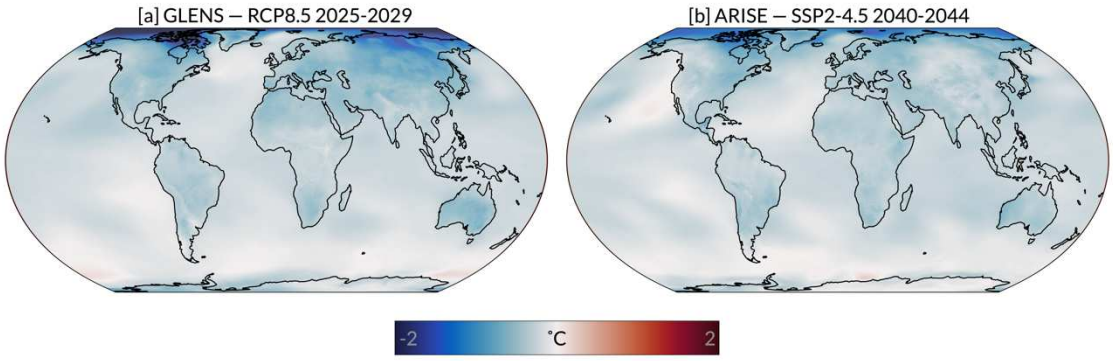


**Figure 6:** Maps of the intervention impact (SAI - no-SAI difference) for annual mean 2m temperature: GLENS [a] and ARISE [b].

In highly localized areas where trends are weak in both the SAI and no-SAI scenarios, the intervention impact is small and noise from internal variability can make it appear as if the intervention has exacerbated warming. This effect can be seen in the very small areas of the Southern Ocean in GLENS (Figure 6a) and the northeastern Pacific Ocean in ARISE (Figure 6b) that display a positively-signed intervention impact. Note that these regional features are not considered robust (Figure C2a, Figure C2b). Internal variability may mask the impact of SAI for

any individual realization, which complicates how the effectiveness of an intervention could be perceived after deployment (Keys et al. 2022).

We connect the averted warming in global mean temperature to implications for the evolution over time of other Earth system variables. Global sea surface temperature (Figure 2c) responds very similarly to global 2m temperature (Figure 2a). Sea ice loss is halted in the Arctic and Antarctic (Figure 2g, Figure 2k) in both GLENS and ARISE. The impact is most dramatic in GLENS; in the no-SAI RCP8.5, the Arctic experiences ice-free minima by mid-century while GLENS keeps sea ice near present-day values. The SAI scenarios have the potential to slow or avert feedbacks involving sea and land ice. Arctic sea ice thickness is maintained alongside sea ice extent (Figure C5), indicating that ice-insulation feedbacks that can cause abrupt sea ice loss (e.g., Burt et al. 2016) could be averted. In Antarctica, halting sea ice loss prevents the exposure of coastal ice shelves to ocean waves which may make land ice less likely to collapse (Massom et al. 2018). Exploring impacts from SAI on the cryosphere in more depth is a clear avenue for future research.

Mid-latitude tropical nights increase drastically in the no-SAI scenarios (Figure 2d) and are associated with the planetary-scale expansion of the tropics (Rajaud & Noblet-Ducoudré 2017). SAI interventions in GLENS and ARISE both halt this process, maintaining tropical nights near their pre-intervention values. Averting increases in tropical nights could mitigate impacts from heat waves, as high overnight temperatures worsen mortality during these events (e.g., Buechley et al. 1972, Laaidi et al. 2012). While heat extremes are mitigated under GLENS or ARISE, extreme cold may be worsened relative to no-SAI climate change scenarios (Tye et al. 2022). More in-depth risk analysis is necessary to quantify tradeoffs in exposure to extreme cold and heat.

Temperature extremes in the ocean are also impacted by the averted warming under SAI. In GLENS and ARISE, increases in marine heatwave frequency are prevented for a point off

the coast of Western Australia (Figure 2l). In the no-SAI scenarios, this location reaches a near-permanent marine heatwave state by mid-century. Marine ecosystems are increasingly affected by compound hazards: combinations of stressors including direct anthropogenic impacts, ocean acidification, and temperature extremes (e.g., Chandrapavan et al. 2019, Gruber et al. 2021). While SAI only mitigates temperature extremes, lessening one component of compound hazards may allow ecosystems to stay within their capacity for resilience (Bernhardt & Leslie 2013).

Precipitation trends in the SAI scenarios oppose the no-SAI climate change response where the sign of the intervention impact (Figure 7) is opposite to that of the snapshot around deployment (Figure 4). Some of the large-scale changes in precipitation opposing the no-SAI climate change trends include the southward shift of the ITCZ, which overcompensates for the northward shift occurring under no-SAI RCP8.5 or no-SAI SSP2-4.5, and the moistening of the Southern Hemisphere subtropics, which opposes subtropical drying. The decrease in precipitation over the west Pacific in GLENS (Figure 7a), in contrast, is of the same sign as in the snapshot around deployment (Figure 4a). This implies that the SAI intervention exacerbates the no-SAI climate change trend in this region. As discussed previously, the decrease in precipitation in this region is responsible for the global decrease in precipitation in GLENS on longer timescales.

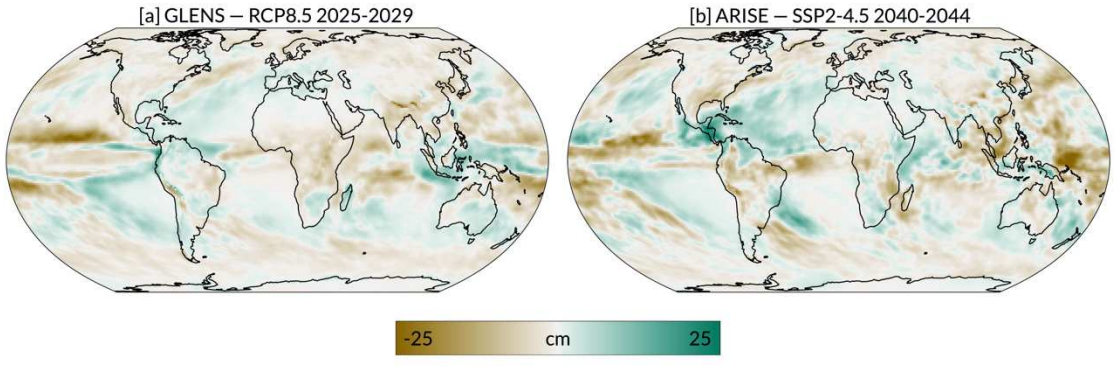


**Figure 7:** Maps of the intervention impact (SAI - no-SAI difference) for annual mean precipitation: GLENS [a] and ARISE [b].

Due to the large internal variability of precipitation (Deser et al. 2012), regional trends are not robust over much of the globe in the decade after deployment (Figure C2c, Figure C2d). Robust regional precipitation responses are particularly difficult to identify in ARISE (Figure C2d), as both the ensemble size and SAI forcing are smaller than in GLENS (Figure C2c). Still, GLENS and ARISE both robustly oppose increases in precipitation in the Arctic that occur in the no-SAI scenarios (Figure 7) associated with rapid warming from Arctic amplification (Figure 2f). Warmer air temperatures support exponentially larger saturation vapor pressures, a trend which is reinforced by increased evaporation from the open ocean due to sea ice loss (Bogerd et al. 2020). Alaska Native communities are highly vulnerable to climate change impacts, particularly those from increased precipitation (Shearer 2012, Melvin et al. 2017). The potential to avert these impacts indicates SAI could mitigate regional climate risk inequality in certain cases, although far more analysis is needed to draw any broader conclusions. Increased temperature and precipitation together yield more vegetation growth in the Arctic (Elmendorf et al. 2012, Dial et al. 2022). Arctic vegetation can exacerbate warming by decreasing surface albedo and increasing local water vapor mixing ratios, which accelerates ice loss and encourages further plant growth (Swann et al. 2010). This positive feedback is considered a possible tipping point in the Earth system (Crump et al. 2021, Heijmans et al. 2022). SAI may prevent this process by preventing increases in temperature and precipitation, although further research would be necessary to examine this in detail.

Globally, GLENS and ARISE both reduce the simple intensity index over land relative to the no-SAI scenarios (Figure 8). Certain robust regional trends (Figure C2e, Figure C2f) are more apparent relative to climate change in the intervention impact than relative to the pre-intervention baseline in the snapshot around deployment. The simple intensity index in East Africa robustly decreases in GLENS and is maintained in ARISE (Figure 2h), while it increases through the period in the no-SAI scenarios. Elsewhere, regional trends in the simple intensity

index are generally not robust. We provide timeseries of the simple intensity index for each IPCC-defined region in Appendix B.

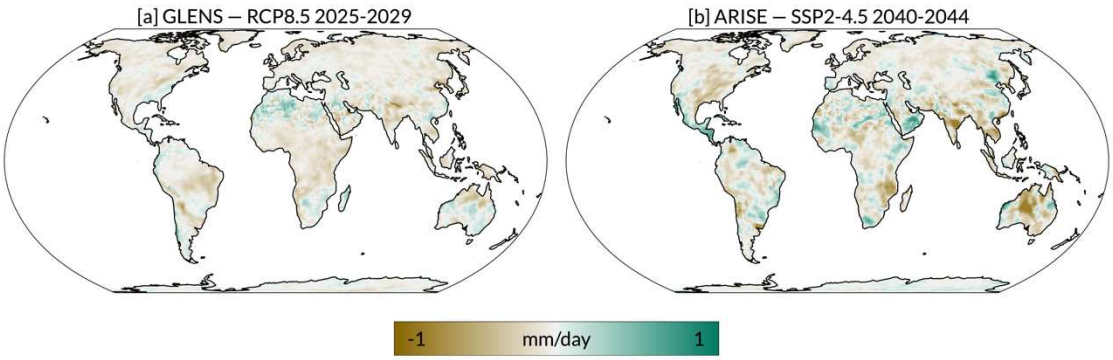


**Figure 8:** Maps of the intervention impact (SAI - no-SAI difference) for annual mean simple intensity index: GLENS [a] and ARISE [b].

## 2.4 CONCLUSIONS

We present two ways to frame output from Earth system modeling experiments with parallel intervention and no-intervention ensemble simulations, which we call the *snapshot around deployment* and the *intervention impact*. Our framings directly address the research questions: "What happens before and after the intervention is deployed in the model?" and "What is the impact of the intervention on a variable relative to climate change with no intervention?" We apply our framings to GLENS and ARISE, the first SAI modeling experiments performed by ensembles of fully-interactive Earth system models. We explore these questions in the decade after SAI deployment, a policy-relevant time horizon that has not been widely explored in the literature with respect to SAI impacts. GLENS and ARISE should not be directly, quantitatively compared to each other due to differences in their experimental designs; thus, we restrict each of our analyses to a single SAI scenario and contrast GLENS and ARISE only in generalities. We use our framings to efficiently describe many aspects of the climate response to SAI, including 2-meter temperature, annual mean precipitation, and the simple intensity index (a measure of precipitation extremes).

Our study is the first to synthesize results from GLENS and ARISE together. We focus on a short-term time horizon of the 10 years after deployment, which is consistent with timescales frequently used by policymakers and planning practitioners to assess climate information (e.g., Bolson et al. 2013, DePolt 2021, Pearman & Cravens 2022, Keys et al. 2022). This differentiates our work from existing literature on the climate response in GLENS or ARISE, which usually examines time horizons later in the century in order to obtain a larger forced signal from the SAI intervention (e.g., Tilmes et al. 2018a, Simpson et al. 2019, Pinto et al. 2020, Camilloni et al. 2022, Richter et al. 2022, Tye et al. 2022). We intend our data analysis to provide a point of entry for researchers or educators unfamiliar with SAI, and include an archive of timeseries depicting each of the variables used with our framings for all IPCC regions (Appendix B).

Our framings can be used with any modeling experiment that has parallel intervention and no-intervention simulations. In particular, we see an opportunity to apply these framings to planned ARISE-SAI experiments that explore a wider variety of temperature targets, deployment dates, and Earth system models (MacMartin et al. 2022). As our framings directly address concrete questions of the climate response to SAI, they could also motivate a more comprehensive regional risk analysis constructed in collaboration with planning practitioners and members of affected communities (e.g., Adelekan & Asiyanbi 2016, DePolt 2021).

We show that while large forced responses to SAI are visible in the ensemble mean within the decade after deployment in GLENS and ARISE, internal variability can mask impacts in individual realizations. The noise from internal variability has important implications for three key open problems highlighted by NASEM (2021): detection, monitoring, and social perception of any climate intervention. Machine learning methods have shown promise for rapid detection of the surface climate response to SAI despite the influence of internal variability (Barnes et al. 2022). Improved understanding of the data most useful to detect SAI could help constrain potential observational platforms for long-term monitoring. Regardless of the true forced

climate response, the noise from internal variability may influence the perceived success or failure of any climate intervention–or climate action more broadly (Keys et al. 2022, Diffenbaugh et al. 2022).

GLENS and ARISE provide high-fidelity depictions of two useful scientific knowledge-building scenarios (Talberg et al. 2018). However, these scenarios are geopolitically idealized: they depict SAI as an uninterrupted worldwide project ("global action" scenarios) with a controller limiting disruptions to global mean climate. Thus, the results from these specific scenarios do not generalize to any given SAI intervention. The large differences between GLENS and ARISE demonstrate that even global action scenarios with many commonalities can produce distinct climate responses, due to factors such as model dependency, the perturbation of the ocean initial conditions, and the direct effects of the underlying greenhouse gas emissions forcing scenario. To explore a scenario of interest, it will be necessary to explicitly model that scenario; the results cannot be assumed to track those of GLENS or ARISE. Future modeling should widely explore the scenario design space, with possible examples of candidates including unilateral ("rogue actor") deployment and environmental peacebuilding (Fitzgerald 2016, Buck 2022).

# CHAPTER 3

# SUMMARY AND FUTURE RESEARCH

## 3.1 SUMMARY OF THESIS

We apply our framings to annual mean 2m temperature, precipitation and the simple intensity index in GLENS and ARISE, which are the first two SAI modeling experiments to use ensembles of Earth system models that comprehensively represent both the aerosol injection process and the climate response. Our work is the first to analyze climate impacts from GLENS and ARISE together. We focus on the time horizon of the first 10 years after SAI deployment, consistent with timescales frequently used by policymakers and planning practitioners to assess climate information. We design our data analysis and visualization to provide a point of entry for researchers and educators new to the subject of climate intervention, and provide an additional archive of timeseries depicting all of the variables used with our framings for each IPCC-defined region (Appendix C).

Our results apply only to the two scenarios of climate intervention modeled here. The GLENS and ARISE scenarios are designed for scientific knowledge-building (Talberg et al. 2018) and depict SAI as an uninterrupted, worldwide project ("global action scenarios") with a controller to limit impacts on the global climate. These strategies are geopolitically idealized–they do not attempt to consider political constraints that would affect the implementation of SAI. The substantial differences between GLENS and ARISE illustrate that even two global action scenarios with many commonalities can produce distinct climate responses.

## 3.2 SURVEY OF FUTURE RESEARCH DIRECTIONS

Our framings could be used to explore the upcoming ARISE experiments planned by NCAR (MacMartin et al., 2022), and are broadly applicable to any experiments using parallel intervention and no-intervention simulations regardless of what kind of intervention is studied.

As our framings directly address concrete questions of the climate response to SAI, they could also motivate a more comprehensive regional risk analysis constructed in collaboration with planning practitioners and members of affected communities (e.g., Adelekan & Asiyanbi 2016, DePolt 2021).

Broader exploration of the space of SAI scenarios will inform discussion of the possible climate responses to different SAI strategies. Future ARISE simulations planned by NCAR will provide detailed insight on the impacts of temperature targets, starting year, interruptions, and phase-out in global-action SAI scenarios with a controller (MacMartin et al. 2022). Modeling of unilateral deployment ("rogue actor" scenarios) would explore the climate implications of geopolitically relevant SAI deployment scenarios (Fitzgerald 2016). Scenarios of environmental peacebuilding may provide new insight on the potential for climate intervention to complement ambitious mitigation strategies (Buck 2022). Developing tools to probe large numbers of scenarios, such as idealized circulation models or nonlinear response machine learning models, could help researchers identify small numbers of candidates to target with resource-intensive Earth system modeling (e.g., Vallis et al. 2018, Mansfield et al. 2020, McGovern et al. 2022).

NASEM (2021) highlighted the rapid detection, long-term monitoring, and public perception of an intervention as key open problems independent of the hypothetical scenario of deployment. Satellite platforms that measure aerosol optical depth would be able to detect SAI within 2 years (Seidel et al. 2014). It would also be straightforward to observe the airplane flights needed to implement SAI at scale (Smith & Wagner 2018). On their own, however, these methods provide little information about the surface climate response. Machine learning has shown promise for detecting the presence of SAI even in highly variable quantities such as temperature extremes and precipitation extremes (Barnes et al. 2022), and could be explored across other variables and spatial scales. Better understanding of the quantities useful for detection of SAI may help constrain platforms for long-term monitoring. Internal variability can

mask the effects of SAI and may lead to the “perceived failure” of any intervention, or climate mitigation policy more generally (Diffenbaugh et al. 2022, Keys et al. 2022). Transdisciplinary social science research can provide insight on effective ways to communicate climate information despite the noise from climate variability.

Many of the processes relevant to SAI, such as middle atmosphere dynamics and aerosol microphysics, are poorly constrained by observations which makes it challenging to evaluate their modeled representations (e.g., SPARC 2022). There are natural analogues to SAI that can provide real-world insight on these Earth system processes without undertaking ethically controversial field experiments (NASEM 2021). Natural analogues include the volcanic emission of sulfate aerosols and the stratospheric injection of smoke by extreme wildfires (e.g., Mills et al. 2017, Das et al. 2021). Additionally, the study of natural analogues provides opportunities for collaboration between the Earth system modeling and observational meteorology communities.

Many fields outside of climate intervention have engaged with relevant questions of ethics and governance. Lessons from the literature in these disciplines, such as renewable energy development, energy policy, and climate adaptation (e.g., Jasanoff 2018, Batres et al. 2021, Leonard 2021), can be applied in the climate intervention community. Engaging with research from these other fields will help us to continue to grow a socially conscious tradition of research in climate intervention.

REFERENCES

Abatzoglou, J. T., Battisti, D. S., Williams, A. P., Hansen, W. D., Harvey, B. J., & Kolden, C. A. (2021). Projected increases in western US forest fire despite growing fuel constraints. *Communications Earth & Environment*, *2*(1), Article 1. https://doi.org/10.1038/s43247-021-00299-0

Adelekan, I. O., & Asiyanbi, A. P. (2016). Flood risk perception in flood-affected communities in Lagos, Nigeria. *Natural Hazards*, *80*(1), 445–469. https://doi.org/10.1007/s11069-015-1977-2

Adhikari, U., Pouyan Nejadhashemi, A., & R. Herman, M. (2015). A Review of Climate Change Impacts on Water Resources in East Africa. *Transactions of the ASABE*, *58*(6), 1493–1507. https://doi.org/10.13031/trans.58.10907

Ainsworth, T. D., Hurd, C. L., Gates, R. D., & Boyd, P. W. (2020). How do we overcome abrupt degradation of marine ecosystems and meet the challenge of heat waves and climate extremes? *Global Change Biology*, *26*(2), 343–354. https://doi.org/10.1111/gcb.14901

Alexander, L. V., Zhang, X., Peterson, T. C., Caesar, J., Gleason, B., Klein Tank, A. M. G., Haylock, M., Collins, D., Trewin, B., Rahimzadeh, F., Tagipour, A., Rupa Kumar, K., Revadekar, J., Griffiths, G., Vincent, L., Stephenson, D. B., Burn, J., Aguilar, E., Brunet, M., … Vazquez-Aguirre, J. L. (2006). Global observed changes in daily climate extremes of temperature and precipitation. *Journal of Geophysical Research: Atmospheres*, *111*(D5). https://doi.org/10.1029/2005JD006290

Ayugi, B., Dike, V., Ngoma, H., Babaousmail, H., Mumo, R., & Ongoma, V. (2021). Future Changes in Precipitation Extremes over East Africa Based on CMIP6 Models. *Water*, *13*(17), Article 17. https://doi.org/10.3390/w13172358

Banerjee, A., Butler, A. H., Polvani, L. M., Robock, A., Simpson, I. R., & Sun, L. (2021). Robust winter warming over Eurasia under stratospheric sulfate geoengineering – the role of stratospheric dynamics. *Atmospheric Chemistry and Physics*, *21*(9), 6985–6997. https://doi.org/10.5194/acp-21-6985-2021

Barnes, E. A., Hurrell, J. W., & Sun, L. (2022). Detecting changes in global extremes under the GLENS-SAI climate intervention strategy. *Geophysical Research Letters*, *n/a*(n/a), e2022GL100198. https://doi.org/10.1029/2022GL100198

Batres, M., Wang, F. M., Buck, H., Kapila, R., Kosar, U., Licker, R., Nagabhushan, D., Rekhelman, E., & Suarez, V. (2021). Environmental and climate justice and technological carbon removal. *The Electricity Journal*, *34*(7), 107002. https://doi.org/10.1016/j.tej.2021.107002

Bednarz, E. M., Visioni, D., Banerjee, A., Braesicke, P., Kravitz, B., & MacMartin, D. G. (2022). The Overlooked Role of the Stratosphere Under a Solar Constant Reduction. *Geophysical Research Letters*, *49*(12), e2022GL098773. https://doi.org/10.1029/2022GL098773

Bednarz, E. M., Visioni, D., MacMartin, D., Kravitz, B., Richter, J. H., & Woodhouse, S. (2022). *Stratospheric Circulation and Ozone Responses from Sulfate Aerosol Injection in CESM Simulations with Different Temperature Targets and Their Impacts on Climate*. American Meteorological Society 102nd Annual Meeting.

Benthuysen, J. A., Oliver, E. C. J., Feng, M., & Marshall, A. G. (2018). Extreme Marine Warming Across Tropical Australia During Austral Summer 2015–2016. *Journal of Geophysical Research: Oceans*, *123*(2), 1301–1326. https://doi.org/10.1002/2017JC013326

Bernhardt, J. R., & Leslie, H. M. (2013). Resilience to climate change in coastal marine ecosystems. *Annual Review of Marine Science*, *5*(1), 371–392.

Bjordal, J., Storelvmo, T., Alterskjær, K., & Carlsen, T. (2020). Equilibrium climate sensitivity above 5 °C plausible due to state-dependent cloud feedback. *Nature Geoscience*, *13*(11), 718–721. https://doi.org/10.1038/s41561-020-00649-1

Bogerd, L., van der Linden, E. C., Krikken, F., & Bintanja, R. (2020). Climate State Dependence of Arctic Precipitation Variability. *Journal of Geophysical Research: Atmospheres*, *125*(8), e2019JD031772. https://doi.org/10.1029/2019JD031772

Bolson, J., Martinez, C., Breuer, N., Srivastava, P., & Knox, P. (2013). Climate information use among southeast US water managers: Beyond barriers and toward opportunities. *Regional Environmental Change*, *13*(1), 141–151. https://doi.org/10.1007/s10113-013-0463-1

Bony, S., Bellon, G., Klocke, D., Sherwood, S., Fermepin, S., & Denvil, S. (2013). Robust direct effect of carbon dioxide on tropical circulation and regional precipitation. *Nature Geoscience*, *6*(6), Article 6. https://doi.org/10.1038/ngeo1799

Boulton, C. A., Lenton, T. M., & Boers, N. (2022). Pronounced loss of Amazon rainforest resilience since the early 2000s. *Nature Climate Change*, *12*(3), Article 3. https://doi.org/10.1038/s41558-022-01287-8

Buck, H. J. (2022). Environmental Peacebuilding and Solar Geoengineering. *Frontiers in Climate*, *4*. https://www.frontiersin.org/article/10.3389/fclim.2022.869774

Buck, H. J., Gammon, A. R., & Preston, C. J. (2014). Gender and Geoengineering. *Hypatia*, *29*(3), 651–669. https://doi.org/10.1111/hypa.12083

Budyko, M. I. (1977). *Climatic Changes*. American Geophysical Union.

Buechley, R. W., Van Bruggen, J., & Truppi, L. E. (1972). Heat island = death island? *Environmental Research*, *5*(1), 85–92. https://doi.org/10.1016/0013-9351(72)90022-9

Burns, E. T., Flegal, J. A., Keith, D. W., Mahajan, A., Tingley, D., & Wagner, G. (2016). What do people think when they think about solar geoengineering? A review of empirical social

science literature, and prospects for future research. *Earth's Future*, *4*(11), 536–542. https://doi.org/10.1002/2016EF000461

Burt, M. A., Randall, D. A., & Branson, M. D. (2016). Dark Warming. *Journal of Climate*, *29*(2), 705–719. https://doi.org/10.1175/JCLI-D-15-0147.1

Camilloni, I., Montroull, N., Gulizia, C., & Saurral, R. I. (2022). La Plata Basin Hydroclimate Response to Solar Radiation Modification With Stratospheric Aerosol Injection. *Frontiers in Climate*, *4*. https://www.frontiersin.org/article/10.3389/fclim.2022.763983

Carr, W. A. (2016). *Vulnerable populations' perspectives on climate engineering* [Ph.D., University of Montana]. http://www.proquest.com/docview/1782319888/abstract/546F9F23A0494EFBPQ/1

Chandrapavan, A., Caputi, N., & Kangas, M. I. (2019). The Decline and Recovery of a Crab Population From an Extreme Marine Heatwave and a Changing Climate. *Frontiers in Marine Science*, *6*. https://www.frontiersin.org/article/10.3389/fmars.2019.00510

Cheng, W., MacMartin, D. G., Kravitz, B., Visioni, D., Bednarz, E. M., Xu, Y., Luo, Y., Huang, L., Hu, Y., Staten, P. W., Hitchcock, P., Moore, J. C., Guo, A., & Deng, X. (2022). Changes in Hadley circulation and intertropical convergence zone under strategic stratospheric aerosol geoengineering. *Npj Climate and Atmospheric Science*, *5*(1), Article 1. https://doi.org/10.1038/s41612-022-00254-6

Ciemer, C., Winkelmann, R., Kurths, J., & Boers, N. (2021). Impact of an AMOC weakening on the stability of the southern Amazon rainforest. *The European Physical Journal Special Topics*, *230*(14), 3065–3073. https://doi.org/10.1140/epjs/s11734-021-00186-x

Crump, S. E., Fréchette, B., Power, M., Cutler, S., de Wet, G., Raynolds, M. K., Raberg, J. H., Briner, J. P., Thomas, E. K., Sepúlveda, J., Shapiro, B., Bunce, M., & Miller, G. H. (2021). Ancient plant DNA reveals High Arctic greening during the Last Interglacial. *Proceedings of the*

*National Academy of Sciences*, *118*(13), e2019069118. https://doi.org/10.1073/pnas.2019069118

Crutzen, P. J. (2006). Albedo Enhancement by Stratospheric Sulfur Injections: A Contribution to Resolve a Policy Dilemma? *Climatic Change*, *77*(3), 211. https://doi.org/10.1007/s10584-006-9101-y

Danabasoglu, G., Lamarque, J.-F., Bacmeister, J., Bailey, D. A., DuVivier, A. K., Edwards, J., Emmons, L. K., Fasullo, J., Garcia, R., Gettelman, A., Hannay, C., Holland, M. M., Large, W. G., Lauritzen, P. H., Lawrence, D. M., Lenaerts, J. T. M., Lindsay, K., Lipscomb, W. H., Mills, M. J., … Strand, W. G. (2020). The Community Earth System Model Version 2 (CESM2). *Journal of Advances in Modeling Earth Systems*, *12*(2), e2019MS001916. https://doi.org/10.1029/2019MS001916

Das, S., Colarco, P. R., Oman, L. D., Taha, G., & Torres, O. (2021). The long-term transport and radiative impacts of the 2017 British Columbia pyrocumulonimbus smoke aerosols in the stratosphere. *Atmospheric Chemistry and Physics*, *21*(15), 12069–12090. https://doi.org/10.5194/acp-21-12069-2021

Depledge, J., Saldivia, M., & Peñasco, C. (2022). Glass half full or glass half empty?: The 2021 Glasgow Climate Conference. *Climate Policy*, *22*(2), 147–157. https://doi.org/10.1080/14693062.2022.2038482

DePolt, K. T. (2021). *Analyzing Drivers of Compound Coastal Water Events (CCWE) with Copulas: A Case Study in Eastern North Carolina*. https://thescholarship.ecu.edu/handle/10342/9730

Deser, C., Phillips, A., Bourdette, V., & Teng, H. (2012). Uncertainty in climate change projections: The role of internal variability. *Climate Dynamics*, *38*(3), 527–546. https://doi.org/10.1007/s00382-010-0977-x

Dial, R. J., Maher, C. T., Hewitt, R. E., & Sullivan, P. F. (2022). Sufficient conditions for rapid range expansion of a boreal conifer. *Nature*, 1–6. https://doi.org/10.1038/s41586-022-05093-2

Diffenbaugh, N. S., Barnes, E. A., & Keys, P. W. (2022). *Probability of continued local-scale warming and extreme events during and after decarbonization*. ResearchSquare. https://doi.org/10.21203/rs.3.rs-1902791/v1

D'Oliveira, F., Melo, F., & Devezas, T. (2016). High-Altitude Platforms—Present Situation and Technology Trends. *Journal of Aerospace Technology and Management*, *8*, 249–262. https://doi.org/10.5028/jatm.v8i3.699

Elmendorf, S. C., Henry, G. H. R., Hollister, R. D., Björk, R. G., Boulanger-Lapointe, N., Cooper, E. J., Cornelissen, J. H. C., Day, T. A., Dorrepaal, E., Elumeeva, T. G., Gill, M., Gould, W. A., Harte, J., Hik, D. S., Hofgaard, A., Johnson, D. R., Johnstone, J. F., Jónsdóttir, I. S., Jorgenson, J. C., … Wipf, S. (2012). Plot-scale evidence of tundra vegetation change and links to recent summer warming. *Nature Climate Change*, *2*(6), Article 6. https://doi.org/10.1038/nclimate1465

Fasullo, J. T. (2020). Evaluating simulated climate patterns from the CMIP archives using satellite and reanalysis datasets using the Climate Model Assessment Tool (CMATv1). *Geoscientific Model Development*, *13*(8), 3627–3642. https://doi.org/10.5194/gmd-13-3627-2020

Fasullo, J. T., & Richter, J. H. (2022, April 14). *Scenario and Model Dependence of Strategic Solar Climate Intervention in CESM* (world) [Preprint]. Earth and Space Science Open Archive; Earth and Space Science Open Archive. https://doi.org/10.1002/essoar.10511096.1

Fasullo, J. T., Tilmes, S., Richter, J. H., Kravitz, B., MacMartin, D. G., Mills, M. J., & Simpson, I. R. (2018). Persistent polar ocean warming in a strategically geoengineered climate. *Nature Geoscience*, *11*(12), Article 12. https://doi.org/10.1038/s41561-018-0249-7

Fischer, E. M., Sippel, S., & Knutti, R. (2021). Increasing probability of record-shattering climate extremes. *Nature Climate Change*, *11*(8), Article 8. https://doi.org/10.1038/s41558-021-01092-9

Fitzgerald, M. (2016). Prison or Precaution: Unilateral, State-Mandated Geoengineering under Principles of International Environmental Law. *New York University Environmental Law Journal*, *24*(2), [i]-282.

Foote, E. (1856). ART. XXXI.—Circumstances affecting the heat of the sun's rays. *American Journal of Science and Arts (1820-1879)*, *22*(66), 382.

Frieler, K., Meinshausen, M., Golly, A., Mengel, M., Lebek, K., Donner, S. D., & Hoegh-Guldberg, O. (2013). Limiting global warming to 2 °C is unlikely to save most coral reefs. *Nature Climate Change*, *3*(2), Article 2. https://doi.org/10.1038/nclimate1674

Gadgil, S., & Rupa Kumar, K. (2006). The Asian monsoon—Agriculture and economy. In *The Asian Monsoon* (pp. 651–683). Springer.

Geen, R., Bordoni, S., Battisti, D. S., & Hui, K. (2020). Monsoons, ITCZs, and the Concept of the Global Monsoon. *Reviews of Geophysics*, *58*(4), e2020RG000700. https://doi.org/10.1029/2020RG000700

Genet, H., McGuire, A. D., Barrett, K., Breen, A., Euskirchen, E. S., Johnstone, J. F., Kasischke, E. S., Melvin, A. M., Bennett, A., Mack, M. C., Rupp, T. S., Schuur, A. E. G., Turetsky, M. R., & Yuan, F. (2013). Modeling the effects of fire severity and climate warming on active layer thickness and soil carbon storage of black spruce forests across the landscape in interior Alaska. *Environmental Research Letters*, *8*(4), 045016. https://doi.org/10.1088/1748-9326/8/4/045016

Gettelman, A., Mills, M. J., Kinnison, D. E., Garcia, R. R., Smith, A. K., Marsh, D. R., Tilmes, S., Vitt, F., Bardeen, C. G., McInerny, J., Liu, H.-L., Solomon, S. C., Polvani, L. M., Emmons, L. K., Lamarque, J.-F., Richter, J. H., Glanville, A. S., Bacmeister, J. T., Phillips, A. S., … Randel,

W. J. (2019). The Whole Atmosphere Community Climate Model Version 6 (WACCM6). *Journal of Geophysical Research: Atmospheres*, *124*(23), 12380–12403. https://doi.org/10.1029/2019JD030943

Groenke, B. (2022). *Pyclimdex* [Python]. https://github.com/bgroenks96/pyclimdex (Original work published 2020)

Gruber, N., Boyd, P. W., Frölicher, T. L., & Vogt, M. (2021). Biogeochemical extremes and compound events in the ocean. *Nature*, *600*(7889), Article 7889. https://doi.org/10.1038/s41586-021-03981-7

Hausfather, Z., & Peters, G. P. (2020). Emissions – the 'business as usual' story is misleading. *Nature*, *577*(7792), 618–620. https://doi.org/10.1038/d41586-020-00177-3

Haywood, J. M., Jones, A., Bellouin, N., & Stephenson, D. (2013). Asymmetric forcing from stratospheric aerosols impacts Sahelian rainfall. *Nature Climate Change*, *3*(7), 660–665. https://doi.org/10.1038/nclimate1857

Heijmans, M. M. P. D., Magnússon, R. Í., Lara, M. J., Frost, G. V., Myers-Smith, I. H., van Huissteden, J., Jorgenson, M. T., Fedorov, A. N., Epstein, H. E., Lawrence, D. M., & Limpens, J. (2022). Tundra vegetation change and impacts on permafrost. *Nature Reviews Earth & Environment*, *3*(1), Article 1. https://doi.org/10.1038/s43017-021-00233-0

Hobday, A. J., Alexander, L. V., Perkins, S. E., Smale, D. A., Straub, S. C., Oliver, E. C. J., Benthuysen, J. A., Burrows, M. T., Donat, M. G., Feng, M., Holbrook, N. J., Moore, P. J., Scannell, H. A., Sen Gupta, A., & Wernberg, T. (2016). A hierarchical approach to defining marine heatwaves. *Progress in Oceanography*, *141*, 227–238. https://doi.org/10.1016/j.pocean.2015.12.014

Holbrook, N., Gupta, A., Oliver, E., Hobday, A., Benthuysen, J., Scannell, H., Smale, D., & Wernberg, T. (2020). Keeping pace with marine heatwaves. *Nature Reviews Earth & Environment*, *1*. https://doi.org/10.1038/s43017-020-0068-4

Hurrell, J. W., Holland, M. M., Gent, P. R., Ghan, S., Kay, J. E., Kushner, P. J., Lamarque, J.-F., Large, W. G., Lawrence, D., Lindsay, K., Lipscomb, W. H., Long, M. C., Mahowald, N., Marsh, D. R., Neale, R. B., Rasch, P., Vavrus, S., Vertenstein, M., Bader, D., … Marshall, S. (2013). The Community Earth System Model: A Framework for Collaborative Research. *Bulletin of the American Meteorological Society*, *94*(9), 1339–1360. https://doi.org/10.1175/BAMS-D-12-00121.1

Iles, C. E., & Hegerl, G. C. (2014). The global precipitation response to volcanic eruptions in the CMIP5 models. *Environmental Research Letters*, *9*(10), 104012. https://doi.org/10.1088/1748-9326/9/10/104012

IPCC. (2021). *Summary for Policymakers* [Climate Change 2021: The Physical Science Basis. Contribution of Working Group I to the Sixth Assessment Report of the Intergovernmental Panel on Climate Change].

Jasanoff, S. (2018). Just transitions: A humble approach to global energy futures. *Energy Research & Social Science*, *35*, 11–14. https://doi.org/10.1016/j.erss.2017.11.025

Jones, A., Haywood, J. M., Alterskjær, K., Boucher, O., Cole, J. N. S., Curry, C. L., Irvine, P. J., Ji, D., Kravitz, B., Egill Kristjánsson, J., Moore, J. C., Niemeier, U., Robock, A., Schmidt, H., Singh, B., Tilmes, S., Watanabe, S., & Yoon, J.-H. (2013). The impact of abrupt suspension of solar radiation management (termination effect) in experiment G2 of the Geoengineering Model Intercomparison Project (GeoMIP). *Journal of Geophysical Research: Atmospheres*, *118*(17), 9743–9752. https://doi.org/10.1002/jgrd.50762

Kang, S. M., Shin, Y., & Xie, S.-P. (2018). Extratropical forcing and tropical rainfall distribution: Energetics framework and ocean Ekman advection. *Npj Climate and Atmospheric Science*, *1*(1), Article 1. https://doi.org/10.1038/s41612-017-0004-6

Kay, J. E., Deser, C., Phillips, A., Mai, A., Hannay, C., Strand, G., Arblaster, J. M., Bates, S. C., Danabasoglu, G., Edwards, J., Holland, M., Kushner, P., Lamarque, J.-F., Lawrence, D., Lindsay, K., Middleton, A., Munoz, E., Neale, R., Oleson, K., … Vertenstein, M. (2015). The Community Earth System Model (CESM) Large Ensemble Project: A Community Resource for Studying Climate Change in the Presence of Internal Climate Variability. *Bulletin of the American Meteorological Society*, *96*(8), 1333–1349. https://doi.org/10.1175/BAMS-D-13-00255.1

Keys, P. W., Barnes, E. A., Diffenbaugh, N. S., Hurrell, J. W., & Bell, C. M. (2022). Potential for perceived failure of stratospheric aerosol injection deployment. *Proceedings of the National Academy of Sciences*, *119*(40), e2210036119. https://doi.org/10.1073/pnas.2210036119

Keys, P. W., Galaz, V., Dyer, M., Matthews, N., Folke, C., Nyström, M., & Cornell, S. E. (2019). Anthropocene risk. *Nature Sustainability*, *2*(8), Article 8. https://doi.org/10.1038/s41893-019-0327-x

King, M. D., Howat, I. M., Candela, S. G., Noh, M. J., Jeong, S., Noël, B. P. Y., van den Broeke, M. R., Wouters, B., & Negrete, A. (2020). Dynamic ice loss from the Greenland Ice Sheet driven by sustained glacier retreat. *Communications Earth & Environment*, *1*(1), Article 1. https://doi.org/10.1038/s43247-020-0001-2

Kintisch, E. (2010). *Hack the planet: Science's best hope-or worst nightmare-for averting climate catastrophe*. John Wiley & Sons.

Kirchmeier-Young, M. C., & Zhang, X. (2020). Human influence has intensified extreme precipitation in North America. *Proceedings of the National Academy of Sciences*, *117*(24), 13308–13313. https://doi.org/10.1073/pnas.1921628117

Kravitz, B., MacMartin, D. G., Mills, M. J., Richter, J. H., Tilmes, S., Lamarque, J.-F., Tribbia, J. J., & Vitt, F. (2017). First Simulations of Designing Stratospheric Sulfate Aerosol Geoengineering to Meet Multiple Simultaneous Climate Objectives. *Journal of Geophysical Research: Atmospheres*, *122*(23), 12,616-12,634. https://doi.org/10.1002/2017JD026874

Kravitz, B., Robock, A., Boucher, O., Schmidt, H., Taylor, K. E., Stenchikov, G., & Schulz, M. (2011). The Geoengineering Model Intercomparison Project (GeoMIP). *Atmospheric Science Letters*, *12*(2), 162–167. https://doi.org/10.1002/asl.316

Kulkarni, A., Gadgil, S., & Patwardhan, S. (2016). Monsoon variability, the 2015 Marathwada drought and rainfed agriculture. *Current Science*, *111*(7), 1182–1193.

Kwiatkowski, L., Cox, P., Halloran, P. R., Mumby, P. J., & Wiltshire, A. J. (2015). Coral bleaching under unconventional scenarios of climate warming and ocean acidification. *Nature Climate Change*, *5*(8), Article 8. https://doi.org/10.1038/nclimate2655

Laaidi, K., Zeghnoun, A., Dousset, B., Bretin, P., Vandentorren, S., Giraudet, E., & Beaudeau, P. (2012). The Impact of Heat Islands on Mortality in Paris during the August 2003 Heat Wave. *Environmental Health Perspectives*, *120*(2), 254–259. https://doi.org/10.1289/ehp.1103532

Leonard, K. (2021). WAMPUM Adaptation framework: Eastern coastal Tribal Nations and sea level rise impacts on water security. *Climate and Development*, *0*(0), 1–10. https://doi.org/10.1080/17565529.2020.1862739

Long, J. C. S., & Shepherd, J. G. (2014). The Strategic Value of Geoengineering Research. In B. Freedman (Ed.), *Global Environmental Change* (pp. 757–770). Springer Netherlands. https://doi.org/10.1007/978-94-007-5784-4_24

MacMartin, D. G., & Kravitz, B. (2019). The Engineering of Climate Engineering. *Annual Review of Control, Robotics, and Autonomous Systems*, *2*(1), 445–467. https://doi.org/10.1146/annurev-control-053018-023725

MacMartin, D. G., Kravitz, B., Keith, D. W., & Jarvis, A. (2014). Dynamics of the coupled human–climate system resulting from closed-loop control of solar geoengineering. *Climate Dynamics*, *43*(1), 243–258. https://doi.org/10.1007/s00382-013-1822-9

MacMartin, D. G., Kravitz, B., Tilmes, S., Richter, J. H., Mills, M. J., Lamarque, J.-F., Tribbia, J. J., & Vitt, F. (2017). The Climate Response to Stratospheric Aerosol Geoengineering Can Be Tailored Using Multiple Injection Locations. *Journal of Geophysical Research: Atmospheres*, *122*(23), 12,574-12,590. https://doi.org/10.1002/2017JD026868

MacMartin, D. G., Visioni, D., Kravitz, B., Richter, J. H., Felgenhauer, T., Lee, W. R., Morrow, D. R., Parson, E. A., & Sugiyama, M. (2022). Scenarios for modeling solar radiation modification. *Proceedings of the National Academy of Sciences*, *119*(33), e2202230119. https://doi.org/10.1073/pnas.2202230119

Maher, N., Milinski, S., & Ludwig, R. (2021). Large ensemble climate model simulations: Introduction, overview, and future prospects for utilising multiple types of large ensemble. *Earth System Dynamics*, *12*(2), 401–418. https://doi.org/10.5194/esd-12-401-2021

Massom, R. A., Scambos, T. A., Bennetts, L. G., Reid, P., Squire, V. A., & Stammerjohn, S. E. (2018). Antarctic ice shelf disintegration triggered by sea ice loss and ocean swell. *Nature*, *558*(7710), 383–389. https://doi.org/10.1038/s41586-018-0212-1

Matthews, H. D., & Wynes, S. (2022). Current global efforts are insufficient to limit warming to 1.5°C. *Science*, *376*(6600), 1404–1409. https://doi.org/10.1126/science.abo3378

Meinshausen, M., Nicholls, Z. R. J., Lewis, J., Gidden, M. J., Vogel, E., Freund, M., Beyerle, U., Gessner, C., Nauels, A., Bauer, N., Canadell, J. G., Daniel, J. S., John, A., Krummel, P. B., Luderer, G., Meinshausen, N., Montzka, S. A., Rayner, P. J., Reimann, S., … Wang, R. H. J. (2020). The shared socio-economic pathway (SSP) greenhouse gas concentrations and their extensions to 2500. *Geoscientific Model Development*, *13*(8), 3571–3605. https://doi.org/10.5194/gmd-13-3571-2020

Melvin, A. M., Larsen, P., Boehlert, B., Neumann, J. E., Chinowsky, P., Espinet, X., Martinich, J., Baumann, M. S., Rennels, L., Bothner, A., Nicolsky, D. J., & Marchenko, S. S. (2017). Climate change damages to Alaska public infrastructure and the economics of proactive adaptation. *Proceedings of the National Academy of Sciences*, *114*(2), E122–E131. https://doi.org/10.1073/pnas.1611056113

MHIWG. (2022). *All about MHWs*. MARINE HEATWAVES. http://www.marineheatwaves.org/all-about-mhws.html

Mills, M. J., Richter, J. H., Tilmes, S., Kravitz, B., MacMartin, D. G., Glanville, A. A., Tribbia, J. J., Lamarque, J.-F., Vitt, F., Schmidt, A., Gettelman, A., Hannay, C., Bacmeister, J. T., & Kinnison, D. E. (2017). Radiative and Chemical Response to Interactive Stratospheric Sulfate Aerosols in Fully Coupled CESM1(WACCM). *Journal of Geophysical Research: Atmospheres*, *122*(23), 13,061-13,078. https://doi.org/10.1002/2017JD027006

Moreno-Chamarro, E., Marshall, J., & Delworth, T. L. (2019). Linking ITCZ Migrations to the AMOC and North Atlantic/Pacific SST Decadal Variability. *Journal of Climate*, *33*(3), 893–905. https://doi.org/10.1175/JCLI-D-19-0258.1

Morgenstern, O., Braesicke, P., Hurwitz, M. M., O'Connor, F. M., Bushell, A. C., Johnson, C. E., & Pyle, J. A. (2008). The World Avoided by the Montreal Protocol. *Geophysical Research Letters*, *35*(16). https://doi.org/10.1029/2008GL034590

Moriyama, R., Sugiyama, M., Kurosawa, A., Masuda, K., Tsuzuki, K., & Ishimoto, Y. (2017). The cost of stratospheric climate engineering revisited. *Mitigation and Adaptation Strategies for Global Change*, *22*(8), 1207–1228. https://doi.org/10.1007/s11027-016-9723-y

NASEM. (2019). *Negative Emissions Technologies and Reliable Sequestration: A Research Agenda*. National Academies of Science, Engineering, and Medicine.

NASEM. (2021). *Reflecting Sunlight: Recommendations for Solar Geoengineering Research and Research Governance*. National Academies of Science, Engineering, and Medicine.

National Research Council. (2015). *Climate Intervention: Reflecting Sunlight to Cool Earth*. National Research Council.

Nicholson, S. E. (2017). Climate and climatic variability of rainfall over eastern Africa. *Reviews of Geophysics*, *55*(3), 590–635. https://doi.org/10.1002/2016RG000544

NSIDC. (2020). *Data: Terminology | National Snow and Ice Data Center*. https://nsidc.org/cryosphere/seaice/data/terminology.html

Oliver, E. (2022). *Marine Heatwaves detection code* [Python]. https://github.com/ecjoliver/marineHeatWaves (Original work published 2015)

Oreskes, N., & Conway, E. M. (2011). *Merchants of Doubt: How a Handful of Scientists Obscured the Truth on Issues from Tobacco Smoke to Global Warming*. Bloomsbury Publishing USA.

Otto, F. E. L. (2017). Attribution of Weather and Climate Events. *Annual Review of Environment and Resources*, *42*(1), 627–646. https://doi.org/10.1146/annurev-environ-102016-060847

Pal, J. S., & Eltahir, E. A. B. (2016). Future temperature in southwest Asia projected to exceed a threshold for human adaptability. *Nature Climate Change*, *6*(2), 197–200. https://doi.org/10.1038/nclimate2833

Panetta, A. M., Stanton, M. L., & Harte, J. (2018). Climate warming drives local extinction: Evidence from observation and experimentation. *Science Advances*, *4*(2), eaaq1819. https://doi.org/10.1126/sciadv.aaq1819

Parkinson, C. L. (2019). A 40-y record reveals gradual Antarctic sea ice increases followed by decreases at rates far exceeding the rates seen in the Arctic. *Proceedings of the National Academy of Sciences*, *116*(29), 14414–14423. https://doi.org/10.1073/pnas.1906556116

Pauw, W. P., Klein, R. J. T., Mbeva, K., Dzebo, A., Cassanmagnago, D., & Rudloff, A. (2018). Beyond headline mitigation numbers: We need more transparent and comparable NDCs to achieve the Paris Agreement on climate change. *Climatic Change*, *147*(1), 23–29. https://doi.org/10.1007/s10584-017-2122-x

Pearman, O., & Cravens, A. E. (2022). Institutional barriers to actionable science: Perspectives from decision support tool creators. *Environmental Science & Policy*, *128*, 317–325. https://doi.org/10.1016/j.envsci.2021.12.004

Philip, S. Y., Kew, S. F., van Oldenborgh, G. J., Anslow, F. S., Seneviratne, S. I., Vautard, R., Coumou, D., Ebi, K. L., Arrighi, J., Singh, R., van Aalst, M., Pereira Marghidan, C., Wehner, M., Yang, W., Li, S., Schumacher, D. L., Hauser, M., Bonnet, R., Luu, L. N., … Otto, F. E. L. (2021). Rapid attribution analysis of the extraordinary heatwave on the Pacific Coast of the US and Canada June 2021. *Earth System Dynamics Discussions*, 1–34. https://doi.org/10.5194/esd-2021-90

Pinto, I., Jack, C., Lennard, C., Tilmes, S., & Odoulami, R. C. (2020). Africa's Climate Response to Solar Radiation Management With Stratospheric Aerosol. *Geophysical Research Letters*, *47*(2), e2019GL086047. https://doi.org/10.1029/2019GL086047

Presidents Science Advisory Committee. (1965). *Restoring the Quality of our Environment*. The White House.

Quaglia, I., Timmreck, C., Niemeier, U., Visioni, D., Pitari, G., Brühl, C., Dhomse, S., Franke, H., Laakso, A., Mann, G., Rozanov, E., & Sukhodolov, T. (2022). Interactive Stratospheric Aerosol models response to different amount and altitude of $SO_2$ injections during the 1991 Pinatubo eruption. *Atmospheric Chemistry and Physics Discussions*, 1–35. https://doi.org/10.5194/acp-2022-514

Rajaud, A., & Noblet-Ducoudré, N. de. (2017). Tropical semi-arid regions expanding over temperate latitudes under climate change. *Climatic Change*, *144*(4), 703–719. https://doi.org/10.1007/s10584-017-2052-7

Rathi, S. K., Sodani, P. R., & Joshi, S. (2021). Summer Temperature and All-cause Mortality from 2006 to 2015 for Smart City Jaipur, India. *Journal of Health Management*, *23*(2), 294–301. https://doi.org/10.1177/09720634211011693

Riahi, K., van Vuuren, D. P., Kriegler, E., Edmonds, J., O'Neill, B. C., Fujimori, S., Bauer, N., Calvin, K., Dellink, R., Fricko, O., Lutz, W., Popp, A., Cuaresma, J. C., Kc, S., Leimbach, M., Jiang, L., Kram, T., Rao, S., Emmerling, J., … Tavoni, M. (2017). The Shared Socioeconomic Pathways and their energy, land use, and greenhouse gas emissions implications: An overview. *Global Environmental Change*, *42*, 153–168. https://doi.org/10.1016/j.gloenvcha.2016.05.009

Richter, H., Jadwiga, Tilmes, S., Glanville, A., Kravitz, B., MacMartin, D. G., Mills, M. J., Simpson, I. R., Vitt, F., Tribbia, J. J., & Lamarque, J.-F. (2018). Stratospheric Response in the First Geoengineering Simulation Meeting Multiple Surface Climate Objectives. *Journal of*

*Geophysical Research: Atmospheres*, *123*(11), 5762–5782. https://doi.org/10.1029/2018JD028285

Richter, J. H., Tilmes, S., Mills, M. J., Tribbia, J. J., Kravitz, B., MacMartin, D. G., Vitt, F., & Lamarque, J.-F. (2017). Stratospheric Dynamical Response and Ozone Feedbacks in the Presence of SO2 Injections. *Journal of Geophysical Research: Atmospheres*, *122*(23), 12,557-12,573. https://doi.org/10.1002/2017JD026912

Richter, J., Visioni, D., MacMartin, D., Bailey, D., Rosenbloom, N., Lee, W., Tye, M., & Lamarque, J.-F. (2022). Assessing Responses and Impacts of Solar climate intervention on the Earth system with stratospheric aerosol injection (ARISE-SAI). *EGUsphere*, 1–35. https://doi.org/10.5194/egusphere-2022-125

Robock, A., Oman, L., & Stenchikov, G. L. (2008). Regional climate responses to geoengineering with tropical and Arctic SO2 injections. *Journal of Geophysical Research: Atmospheres*, *113*(D16). https://doi.org/10.1029/2008JD010050

Rugenstein, M. A. A., Gregory, J. M., Schaller, N., Sedláček, J., & Knutti, R. (2016). Multiannual Ocean–Atmosphere Adjustments to Radiative Forcing. *Journal of Climate*, *29*(15), 5643–5659. https://doi.org/10.1175/JCLI-D-16-0312.1

Seidel, D. J., Feingold, G., Jacobson, A. R., & Loeb, N. (2014). Detection limits of albedo changes induced by climate engineering. *Nature Climate Change*, *4*(2), 93–98. https://doi.org/10.1038/nclimate2076

Shearer, C. (2012). The Social Construction of Alaska Native Vulnerability to Climate Change. *Race, Gender & Class*, *19*(1/2), 61–79.

Sherwood, S. C., Bony, S., Boucher, O., Bretherton, C., Forster, P. M., Gregory, J. M., & Stevens, B. (2015). Adjustments in the Forcing-Feedback Framework for Understanding Climate Change. *Bulletin of the American Meteorological Society*, *96*(2), 217–228. https://doi.org/10.1175/BAMS-D-13-00167.1

Sillmann, J., & Roeckner, E. (2008). Indices for extreme events in projections of anthropogenic climate change. *Climatic Change*, *86*(1), 83–104. https://doi.org/10.1007/s10584-007-9308-6

Simpson, I. R., Tilmes, S., Richter, J. H., Kravitz, B., MacMartin, D. G., Mills, M. J., Fasullo, J. T., & Pendergrass, A. G. (2019). The Regional Hydroclimate Response to Stratospheric Sulfate Geoengineering and the Role of Stratospheric Heating. *Journal of Geophysical Research: Atmospheres*, *124*(23), 12587–12616. https://doi.org/10.1029/2019JD031093

Smith, K. E., Burrows, M. T., Hobday, A. J., Sen Gupta, A., Moore, P. J., Thomsen, M., Wernberg, T., & Smale, D. A. (2021). Socioeconomic impacts of marine heatwaves: Global issues and opportunities. *Science*, *374*(6566), eabj3593. https://doi.org/10.1126/science.abj3593

Smith, W., Bhattarai, U., Bingaman, D. C., Mace, J. L., & Rice, C. V. (2022). Review of possible very high-altitude platforms for stratospheric aerosol injection. *Environmental Research Communications*, *4*(3), 031002. https://doi.org/10.1088/2515-7620/ac4f5d

Smith, W., & Wagner, G. (2018). Stratospheric aerosol injection tactics and costs in the first 15 years of deployment. *Environmental Research Letters*, *13*(12), 124001. https://doi.org/10.1088/1748-9326/aae98d

Song, H., Kemp, D. B., Tian, L., Chu, D., Song, H., & Dai, X. (2021). Thresholds of temperature change for mass extinctions. *Nature Communications*, *12*(1), 4694. https://doi.org/10.1038/s41467-021-25019-2

SPARC. (2022). *SPARC Reanalysis Intercomparison Project (S-RIP) Final Report* (No. 10). World Climate Research Programme. http://www.sparc-climate.org/publications/sparc-reports

Stroeve, J. C., Serreze, M. C., Holland, M. M., Kay, J. E., Malanik, J., & Barrett, A. P. (2012). The Arctic's rapidly shrinking sea ice cover: A research synthesis. *Climatic Change*, *110*(3), 1005–1027. https://doi.org/10.1007/s10584-011-0101-1

Swann, A. L., Fung, I. Y., Levis, S., Bonan, G. B., & Doney, S. C. (2010). Changes in Arctic vegetation amplify high-latitude warming through the greenhouse effect. *Proceedings of the National Academy of Sciences*, *107*(4), 1295–1300. https://doi.org/10.1073/pnas.0913846107

Talberg, A., Thomas, S., Christoff, P., & Karoly, D. (2018). How geoengineering scenarios frame assumptions and create expectations. *Sustainability Science*, *13*(4), 1093–1104. https://doi.org/10.1007/s11625-018-0527-8

Tebaldi, C., Dorheim, K., Wehner, M., & Leung, R. (2021). Extreme metrics from large ensembles: Investigating the effects of ensemble size on their estimates. *Earth System Dynamics*, *12*(4), 1427–1501. https://doi.org/10.5194/esd-12-1427-2021

The Royal Society. (2009). *Geoengineering the Climate*.

Tilmes, S., Richter, J. H., Kravitz, B., MacMartin, D. G., Mills, M. J., Simpson, I. R., Glanville, A. S., Fasullo, J. T., Phillips, A. S., Lamarque, J.-F., Tribbia, J., Edwards, J., Mickelson, S., & Ghosh, S. (2018). CESM1(WACCM) Stratospheric Aerosol Geoengineering Large Ensemble Project. *Bulletin of the American Meteorological Society*, *99*(11), 2361–2371. https://doi.org/10.1175/BAMS-D-17-0267.1

Tilmes, S., Richter, J. H., Mills, M. J., Kravitz, B., MacMartin, D. G., Garcia, R. R., Kinnison, D. E., Lamarque, J.-F., Tribbia, J., & Vitt, F. (2018). Effects of Different Stratospheric SO2 Injection Altitudes on Stratospheric Chemistry and Dynamics. *Journal of Geophysical Research: Atmospheres*, *123*(9), 4654–4673. https://doi.org/10.1002/2017JD028146

Tilmes, S., Richter, J. H., Mills, M. J., Kravitz, B., MacMartin, D. G., Vitt, F., Tribbia, J. J., & Lamarque, J.-F. (2017). Sensitivity of Aerosol Distribution and Climate Response to Stratospheric SO2 Injection Locations. *Journal of Geophysical Research: Atmospheres*, *122*(23), 12,591-12,615. https://doi.org/10.1002/2017JD026888

Timmreck, C. (2012). Modeling the climatic effects of large explosive volcanic eruptions. *WIREs Climate Change*, *3*(6), 545–564. https://doi.org/10.1002/wcc.192

Timmreck, C., Mann, G. W., Aquila, V., Hommel, R., Lee, L. A., Schmidt, A., Brühl, C., Carn, S., Chin, M., Dhomse, S. S., Diehl, T., English, J. M., Mills, M. J., Neely, R., Sheng, J., Toohey, M., & Weisenstein, D. (2018). The Interactive Stratospheric Aerosol Model Intercomparison Project (ISA-MIP): Motivation and experimental design. *Geoscientific Model Development*, *11*(7), 2581–2608. https://doi.org/10.5194/gmd-11-2581-2018

Tomkins, L. M., Yuter, S. E., Miller, M. A., & Allen, L. R. (2022). Image Muting of Mixed Precipitation to Improve Identification of Regions of Heavy Snow in Radar Data. *Atmospheric Measurement Techniques*, 1–15. https://doi.org/10.5194/amt-2022-160

Trisos, C. H., Amatulli, G., Gurevitch, J., Robock, A., Xia, L., & Zambri, B. (2018). Potentially dangerous consequences for biodiversity of solar geoengineering implementation and termination. *Nature Ecology & Evolution*, *2*(3), Article 3. https://doi.org/10.1038/s41559-017-0431-0

Tye, M. R., Dagon, K., Molina, M. J., Richter, J. H., Visioni, D., Kravitz, B., & Tilmes, S. (2022). Indices of extremes: Geographic patterns of change in extremes and associated vegetation impacts under climate intervention. *Earth System Dynamics*, *13*(3), 1233–1257. https://doi.org/10.5194/esd-13-1233-2022

Undorf, S., Polson, D., Bollasina, M. A., Ming, Y., Schurer, A., & Hegerl, G. C. (2018). Detectable Impact of Local and Remote Anthropogenic Aerosols on the 20th Century Changes of West African and South Asian Monsoon Precipitation. *Journal of Geophysical Research: Atmospheres*, *123*(10), 4871–4889. https://doi.org/10.1029/2017JD027711

UNFCCC. (2016). Paris Agreement. *International Legal Materials*, *55*(4), 743–755.

United Nations. (2021). *Secretary-General's statement on the IPCC Working Group 1 Report on the Physical Science Basis of the Sixth Assessment | United Nations Secretary-General*.

https://www.un.org/sg/en/content/secretary-generals-statement-the-ipcc-working-group-1-report-the-physical-science-basis-of-the-sixth-assessment

USGCRP. (2018). *Fourth National Climate Assessment* (No. 4). United States Global Change Research Program.

van Oldenborgh, G. J., Collins, M., Arblaster, J., Christensen, J. H., Marotzke, J., Power, S. B., Rummukainen, M., & Zhou, T. (2013). *Annex I: Atlas of Global and Regional Climate Projections* (T. F. Stocker, D. Qin, G.-K. Plattner, M. M. B. Tignor, S. K. Allen, J. Boschung, A. Nauels, Y. Xia, V. Bex, & P. M. Midgley, Eds.; pp. 1311–1393). Cambridge University Press. https://www.ipcc.ch/report/ar5/wg1/

van Vuuren, D. P., Edmonds, J., Kainuma, M., Riahi, K., Thomson, A., Hibbard, K., Hurtt, G. C., Kram, T., Krey, V., Lamarque, J.-F., Masui, T., Meinshausen, M., Nakicenovic, N., Smith, S. J., & Rose, S. K. (2011). The representative concentration pathways: An overview. *Climatic Change*, *109*(1), 5. https://doi.org/10.1007/s10584-011-0148-z

Visioni, D., MacMartin, D. G., & Kravitz, B. (2021). Is Turning Down the Sun a Good Proxy for Stratospheric Sulfate Geoengineering? *Journal of Geophysical Research: Atmospheres*, *126*(5), e2020JD033952. https://doi.org/10.1029/2020JD033952

Wainwright, C. M., Finney, D. L., Kilavi, M., Black, E., & Marsham, J. H. (2021). Extreme rainfall in East Africa, October 2019–January 2020 and context under future climate change. *Weather*, *76*(1), 26–31. https://doi.org/10.1002/wea.3824

Weldeab, S., Schneider, R. R., Yu, J., & Kylander-Clark, A. (2022). Evidence for massive methane hydrate destabilization during the penultimate interglacial warming. *Proceedings of the National Academy of Sciences*, *119*(35), e2201871119. https://doi.org/10.1073/pnas.2201871119

Wigley, T. M. L. (2006). A Combined Mitigation/Geoengineering Approach to Climate Stabilization. *Science*. https://doi.org/10.1126/science.1131728

Zhang, X., Alexander, L., Hegerl, G. C., Jones, P., Tank, A. K., Peterson, T. C., Trewin, B., & Zwiers, F. W. (2011). Indices for monitoring changes in extremes based on daily temperature and precipitation data. *WIREs Climate Change*, *2*(6), 851–870. https://doi.org/10.1002/wcc.147

Zhang, Y., MacMartin, D. G., Visioni, D., & Kravitz, B. (2022). How large is the design space for stratospheric aerosol geoengineering? *Earth System Dynamics*, *13*(1), 201–217. https://doi.org/10.5194/esd-13-201-2022

APPENDIX A

ROBUSTNESS

We define a metric called *robustness* to quantify where the signal from the forced response to SAI is large relative to noise from internal variability and the response to climate change. The use of robustness is enabled by GLENS and ARISE containing parallel SAI and no-SAI ensemble simulations. Described qualitatively, robustness is the number of SAI realizations whose time mean falls outside (exceeds or subceeds) a chosen quantity of time means of no-SAI realizations for a given time period at a point. A variable that showed perfect robustness would have each SAI ensemble member fall outside the chosen quantity of no-SAI realizations every time. More formally, robustness can be described mathematically as the following statement:

$$\rho_{\theta,\phi} = \max\left(\left\{\mathrm{n}\left(r_{S_{\theta,\phi r_t} > \overline{\tilde{S}_{\theta,\phi r_{\{B\}}}}}\right), \mathrm{n}\left(r_{S_{\theta,\phi r_t} < \overline{\tilde{S}_{\theta,\phi r_{\{B\}}}}}\right)\right\}, \left| \forall t \in \{0, \ldots, z\} \right.\right)$$

In this equation, $\boldsymbol{\rho_{\theta,\phi}}$ denotes the robustness at some longitude and latitude. $\overline{\boldsymbol{S_{\theta,\phi r_t}}}$ is the time mean over a given period for a variable at some longitude $\boldsymbol{\theta}$ and latitude $\boldsymbol{\phi}$ for each SAI realization $r_t$, $\overline{\tilde{S}_{\boldsymbol{\theta,\phi r_{\{B\}}}}}$ denotes time means of a variable at a longitude $\boldsymbol{\theta}$ and latitude $\boldsymbol{\phi}$ for $\boldsymbol{B}$ number of no-SAI realizations $r_{\{B\}}$, and $\boldsymbol{z}$ is the size of the SAI ensemble. The robustness calculation is repeated for every latitude and longitude to generate a map of robustness for a given variable. The unit of robustness is "number of ensemble members" as inherited from the cardinality operator n(). Robustness is always non-negative and can never be larger than the size of the SAI ensemble, i.e. $\boldsymbol{\rho_{\theta,\phi}} = z$ is the upper bound for robustness.

Robustness is shown for each variable analyzed in the text in Figure C2. The maximum values for robustness are 21 ensemble members in GLENS and 10 ensemble members in ARISE. We consider regions where robustness is greater than 13 members (GLENS) or 7

members (ARISE) to be "robust." In Figure C2, robustness can be assessed visually by interpreting areas colored in green or yellow as being robust, while grayscale colors ("muted" regions, Tomkins et al. 2022) are not robust. However, we emphasize that the choice of threshold is subjective. We encourage interested readers to assess results to their own standard using Figure C2.

The algorithm to calculate robustness is detailed here. In the archive accompanying this thesis, robustness is implemented in the module fun_robustness.py.

1. Choose the time period of interest. We define this time period as 2025-2029 for GLENS and 2040-2044 for ARISE.
2. The user defines the value *B*. A given SAI member must exceed or subceed this number of no-SAI members to be considered to have a robust signal. The value of *B* and the time period of interest are the only user choices required to calculate robustness. We set *B* equal to 11 for GLENS and 6 for ARISE given their differing ensemble sizes.
3. Choose a realization from the SAI ensemble.
4. Compare the mean value of the given SAI member during the time period to the mean values from the corresponding time period of every no-SAI member. Calculate the number of no-SAI realizations that the SAI member exceeds and subceeds. These two numbers are retained as $G_{exc}$ and $G_{sub}$.
5. Repeat steps 3 and 4 for each SAI member. In this way, each SAI member will be compared to every no-SAI realization.
6. The number of SAI realizations surpassing *B* is summed for each of $G_{exc}$ and $G_{sub}$ ensuring both negative- and positive-signed forced responses from SAI can be captured. Mathematically, this describes the calculation of $\left(\left\{\mathrm{n}\left(r_{S_{\theta,\phi r_t} > \overline{\tilde{S}_{\theta,\phi r_{\{B\}}}}}\right), \mathrm{n}\left(r_{S_{\theta,\phi r_t} < \overline{\tilde{S}_{\theta,\phi r_{\{B\}}}}}\right)\right\}, \middle| \forall t \in \{0, \ldots, z\}\right.$ in the equation provided earlier.

7. The maximum of the two numbers from the previous step is the *robustness* at the given grid point and time period.
8. The calculation is repeated for every grid point to generate a map of robustness.

# APPENDIX B

## ARCHIVE OF TIMESERIES

In order to comprehensively illustrate the regional climate response in GLENS and ARISE, we provide timeseries for annual 2m temperature, annual precipitation, and the simple intensity index at all IPCC WG1-AR5 regions. These figures are located at the following archive hosted by the Open Science Foundation: doi.org/10.17605/OSF.IO/TEV3R. This archive also contains the Python code necessary to calculate the robustness metric described in Appendix A.

In the figures in this archive, GLENS is referred to as “GLENS-SAI” and ARISE as “ARISE-SAI-1.5.” These full names provide additional clarity on the experiments used in the figures in case readers encounter these images out of context.

# APPENDIX C

## SUPPLEMENTARY FIGURES

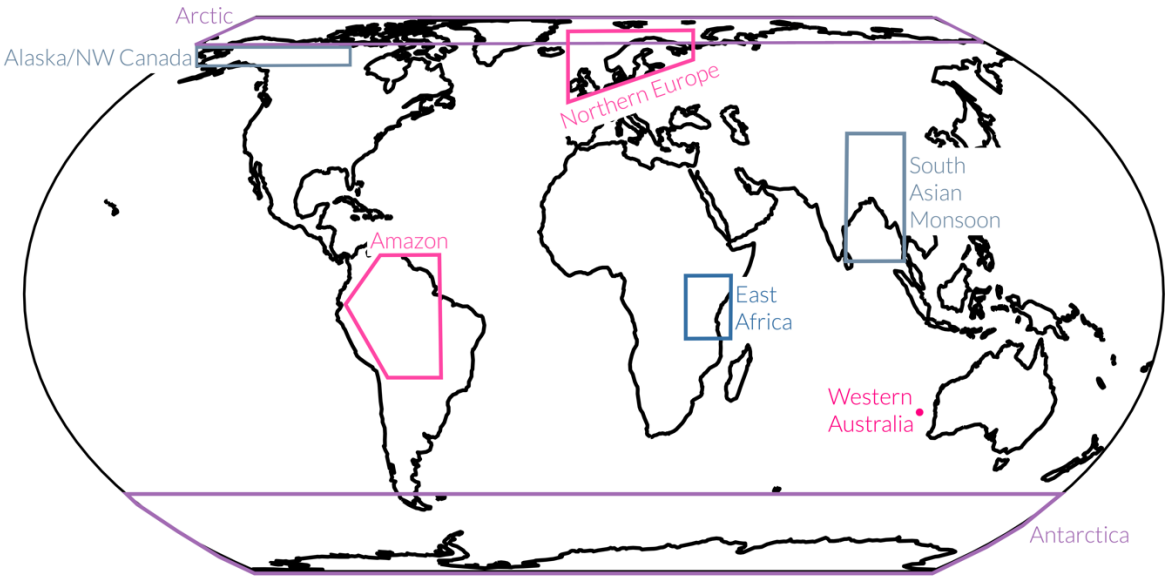


**Figure C1:** Regions used for panels in Figure 8. Definitions are from IPCC (2013), except for East Africa (Ayugi et al. 2021), South Asian Monsoon (Geen et al. 2020), and Western Australia (Hobday et al. 2016).

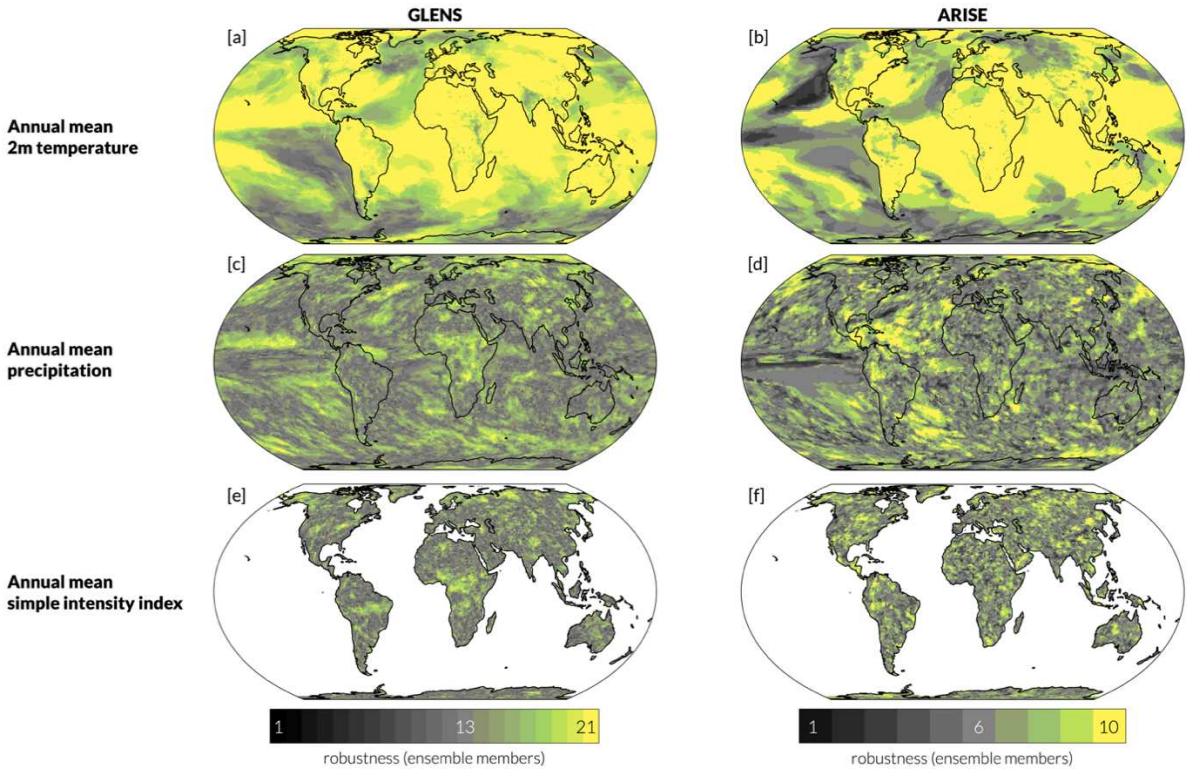


**Figure C2:** Robustness of data shown in Figures 1-7. See Appendix A for definition of robustness.

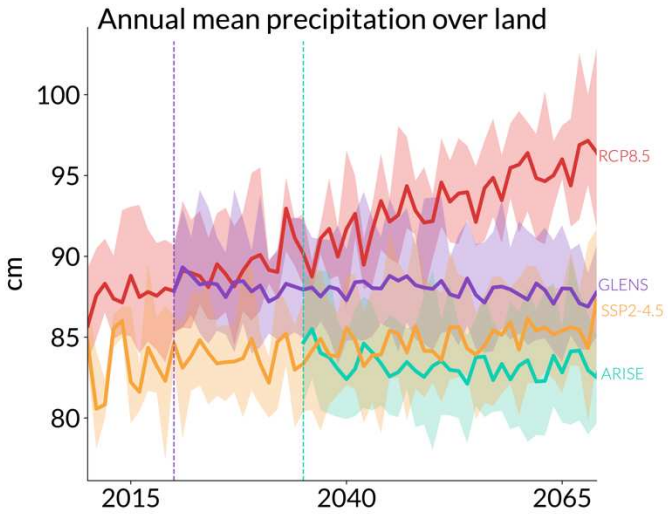


**Figure C3:** Timeseries of annual mean precipitation over land only in GLENS and ARISE.

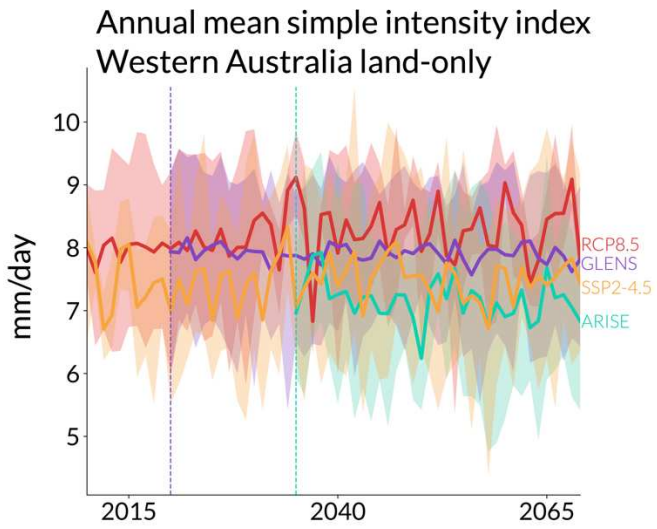


**Figure C4:** Timeseries of simple intensity index for land-only Western Australia. Region definition: 38˚S to 11˚S, 112˚E to 136˚E.

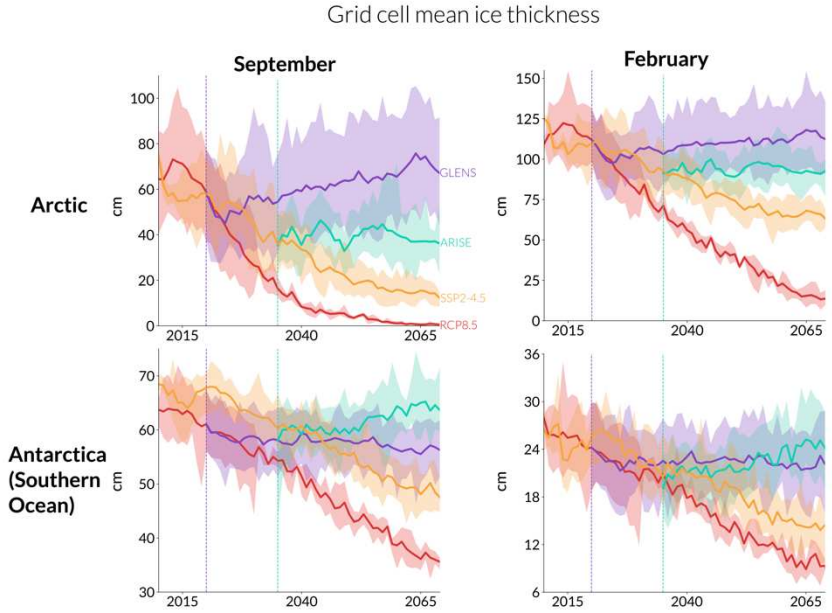


**Figure C5:** Timeseries of grid cell mean sea ice thickness in GLENS and ARISE.